A B

C1

EUROPEAN ORGANIZATION FOR NUCLEAR RESEARCH

CERN LIBRARIES, GENEVA
P00021347

CERN-PPE/94-24

9 February 1994

SW9408

A Precision Measurement of the Average Lifetime of B Hadrons

DELPHI Collaboration

Abstract

The average lifetime of B hadrons was measured using data collected with the DELPHI detector at the LEP collider during 1991 and 1992. The measurement was performed using two different analyses. The first method was an improvement on a previous technique, which used charged particle impact parameter distributions. This analysis measured an average lifetime for B hadrons of

$$\tau_B = 1.542 \pm 0.021 \text{ (stat.)} \pm 0.045 \text{ (syst.)} \text{ ps.}$$

The second method was based on a new technique, which used inclusively reconstructed secondary vertices to measure

$$\tau_B = 1.599 \pm 0.014 \text{ (stat.)} \pm 0.035 \text{ (syst.)} \text{ ps.}$$

Taking into account both the statistical and systematic correlations, the results of these two methods were combined to give an average lifetime for B hadrons of

$$\tau_B = 1.582 \pm 0.012 \text{ (stat.)} \pm 0.032 \text{ (syst.)} \text{ ps.}$$

(To be submitted to Zeit. Phys. C)

P.Abreu[20], W.Adam[7], T.Adye[37], E.Agasi[30], R.Aleksan[39], G.D.Alekseev[14], P.Allport[21], S.Almehed[23], F.M.L.Almeida Junior[47], S.J.Alvsvaag[4], U.Amaldi[7], A.Andreazza[27], P.Antilogus[24], W-D.Apel[15], R.J.Apsimon[37], Y.Arnoud[39], B.Åsman[44], J-E.Augustin[18], A.Augustinus[30], P.Baillon[7], P.Bambade[18], F.Barao[20], R.Barate[12], G.Barbiellini[46], D.Y.Bardin[14], G.J.Barker[34], A.Baroncelli[40], O.Barring[7], J.A.Barrio[25], W.Bartl[50], M.J.Bates[37], M.Battaglia[13], M.Baubillier[22], K-H.Becks[52], M.Begalli[36], P.Beilliere[6], Yu.Belokopytov[42], P.Beltran[9], A.C.Benvenuti[5], M.Berggren[18], D.Bertrand[2], F.Bianchi[45], M.Bigi[45], M.S.Bilenky[14], P.Billoir[22], J.Bjarne[23], D.Bloch[8], J.Blocki[51], S.Blyth[34], V.Bocci[38], P.N.Bogolubov[14], T.Bolognese[39], M.Bonesini[27], W.Bonivento[27], P.S.L.Booth[21], G.Borisov[42], C.Bosio[40], B.Bostjancic[43], S.Bosworth[34], O.Botner[48], B.Bouquet[18], C.Bourdarios[18], T.J.V.Bowcock[21], M.Bozzo[11], S.Braibant[2], P.Branchini[40], K.D.Brand[35], R.A.Brenner[13], H.Briand[22], C.Bricman[2], L.Brillault[22], R.C.A.Brown[7], J-M.Brunet[6], L.Bugge[32], T.Buran[32], A.Buys[7], J.A.M.A.Buytaert[7], M.Caccia[27], M.Calvi[27], A.J.Camacho Rozas[41], R.Campion[21], T.Camporesi[7], V.Canale[38], K.Cankocak[44], F.Cao[2], F.Carena[7], P.Carrilho[47], L.Carroll[21], R.Cases[49], C.Caso[11], M.V.Castillo Gimenez[49], A.Cattai[7], F.R.Cavallo[5], L.Cerrito[38], V.Chabaud[7], A.Chan[1], Ph.Charpentier[7], J.Chauveau[22], P.Checchia[35], G.A.Chelkov[14], L.Chevalier[39], P.Chliapnikov[42], V.Chorowicz[22], J.T.M.Chrin[49], V.Cindro[43], P.Collins[34], J.L.Contreras[18], R.Contri[11], E.Cortina[49], G.Cosme[18], F.Couchot[18], H.B.Crawley[1], D.Crennell[37], G.Crosetti[11], J.Cuevas Maestro[33], S.Czellar[13], E.Dahl-Jensen[28], J.Dahm[52], B.Dalmagne[18], M.Dam[32], G.Damgaard[28], E.Daubie[2], A.Daum[15], P.D.Dauncey[7], M.Davenport[7], J.Davies[21], W.Da Silva[22], C.Defoix[6], P.Delpierre[26], N.Demaria[34], A.De Angelis[7], H.De Boeck[2], W.De Boer[15], S.De Brabandere[2], C.De Clercq[2], M.D.M.De Fez Laso[49], C.De La Vaissiere[22], B.De Lotto[46], A.De Min[27], L.De Paula[47], H.Dijkstra[7], L.Di Ciaccio[38], F.Djama[8], J.Dolbeau[6], M.Donszelmann[7], K.Doroba[51], M.Dracos[8], J.Drees[52], M.Dris[31], Y.Dufour[7], F.Dupont[12], D.Edsall[1], L-O.Eek[48], R.Ehret[15], T.Ekelof[48], G.Ekspong[44], A.Elliot Peisert[7], M.Elsing[52], J-P.Engel[8], N.Ershaidat[22], M.Espirito Santo[20], V.Falaleev[42], D.Fassouliotis[31], M.Feindt[7], A.Fenyuk[42], A.Ferrer[49], T.A.Filippas[31], A.Firestone[1], H.Foeth[7], E.Fokitis[31], F.Fontanelli[11], K.A.J.Forbes[21], F.Formenti[7], J-L.Fousset[26], S.Francon[24], B.Franek[37], P.Frenkiel[6], D.C.Fries[15], A.G.Frodesen[4], R.Fruhwirth[50], F.Fulda-Quenzer[18], H.Furstenau[7], J.Fuster[7], D.Gamba[45], M.Gandelman[17], C.Garcia[49], J.Garcia[41], C.Gaspar[7], U.Gasparini[35], Ph.Gavillet[7], E.N.Gazis[31], J-P.Gerber[8], P.Giacomelli[7], D.Gillespie[7], R.Gokieli[51], B.Golob[43], V.M.Golovatyuk[14], J.J.Gomez Y Cadenas[7], G.Gopal[37], L.Gorn[1], M.Gorski[51], V.Gracco[11], F.Grard[2], E.Graziani[40], G.Grosdidier[18], B.Grossetete[22], P.Gunnarsson[44], J.Guy[37], U.Haedinger[15], F.Hahn[52], M.Hahn[44], S.Hahn[52], S.Haider[30], Z.Hajduk[16], A.Hakansson[23], A.Hallgren[48], K.Hamacher[52], G.Hamel De Monchenault[39], W.Hao[30], F.J.Harris[34], V.Hedberg[23], R.Henriques[20], J.J.Hernandez[49], J.A.Hernando[49], P.Herquet[2], H.Herr[7], T.L.Hessing[21], C.O.Higgins[21], E.Higon[49], H.J.Hilke[7], T.S.Hill[1], S.D.Hodgson[34], T.Hofmokl[51], S-O.Holmgren[44], P.J.Holt[34], D.Holthuizen[30], P.F.Honore[6], M.Houlden[21], J.Hrubec[50], K.Huet[2], K.Hultqvist[44], P.Ioannou[3], P-S.Iversen[4], J.N.Jackson[21], R.Jacobsson[44], P.Jalocha[16], G.Jarlskog[23], P.Jarry[39], B.Jean-Marie[18], E.K.Johansson[44], M.Jonker[7], L.Jonsson[23], P.Juillot[8], M.Kaiser[15], G.Kalkanis[3], G.Kalmus[37], F.Kapusta[22], M.Karlsson[44], E.Karvelas[9], S.Katsanevas[3], E.C.Katsoufis[31], R.Keranen[7], B.A.Khomenko[14], N.N.Khovanski[14], B.King[21], N.J.Kjaer[28], H.Klein[7], A.Klovning[4], P.Kluit[30], A.Koch-Mehrin[52], J.H.Koehne[15], B.Koene[30], P.Kokkinias[9], M.Koratzinos[32], K.Korcyl[16], A.V.Korytov[14], V.Kostioukhine[42], C.Kourkoumelis[3], O.Kouznetsov[14], P.H.Kramer[52], M.Krammer[50], C.Kreuter[15], J.Krolikowski[51], I.Kronkvist[23], W.Krupinski[16], K.Kulka[48], K.Kurvinen[13], C.Lacasta[49], C.Lambropoulos[9], J.W.Lamsa[1], L.Lanceri[46], P.Langefeld[52], V.Lapin[42], I.Last[21], J-P.Laugier[39], R.Lauhakangas[13], G.Leder[50], F.Ledroit[12], R.Leitner[29], Y.Lemoigne[39], J.Lemonne[2], G.Lenzen[52], V.Lepeltier[18], T.Lesiak[16], J.M.Levy[8], E.Lieb[52], D.Liko[50], R.Lindner[52], A.Lipniacka[18], I.Lippi[35], B.Loerstad[23], M.Lokajicek[10], J.G.Loken[34], A.Lopez-Fernandez[7], M.A.Lopez Aguera[41], M.Los[30], D.Loukas[9], J.J.Lozano[49], P.Lutz[6], L.Lyons[34], G.Maehlum[15], J.Maillard[6], A.Maio[20], A.Maltezos[9], F.Mandl[50], J.Marco[41], B.Marechal[47], M.Margoni[35], J-C.Marin[7], C.Mariotti[40], A.Markou[9], T.Maron[52], S.Marti[49], C.Martinez-Rivero[41], F.Martinez-Vidal[49], F.Matorras[41], C.Matteuzzi[27], G.Matthiae[38], M.Mazzucato[35], M.Mc Cubbin[21], R.Mc Kay[1], R.Mc Nulty[21], J.Medbo[48], C.Meroni[27], W.T.Meyer[1], M.Michelotto[35], E.Migliore[45], I.Mikulec[50], L.Mirabito[24], W.A.Mitaroff[50], G.V.Mitselmakher[14], U.Mjoernmark[23], T.Moa[44], R.Moeller[28], K.Moenig[7], M.R.Monge[11], P.Morettini[11], H.Mueller[15], W.J.Murray[37], B.Muryn[16], G.Myatt[34], F.Naraghi[12], F.L.Navarria[5], P.Negri[27], S.Nemecek[10], W.Neumann[52], N.Neumeister[50], R.Nicolaidou[3], B.S.Nielsen[28], V.Nikolaenko[42], P.E.S.Nilsen[4], P.Niss[44], A.Nomerotski[35], M.Novak[10], V.Obraztsov[42], A.G.Olshevski[14], R.Orava[13], A.Ostankov[42], K.Osterberg[13], A.Ouraou[39], P.Paganini[18], M.Paganoni[27], R.Pain[22], H.Palka[16], Th.D.Papadopoulou[31], L.Pape[7], F.Parodi[11], A.Passeri[40], M.Pegoraro[35], J.Pennanen[13], L.Peralta[20], V.Perevozchikov[42], H.Pernegger[50], A.Perrotta[5], C.Petridou[46], A.Petrolini[11], G.Piana[11], F.Pierre[39], M.Pimenta[20], S.Plaszczynski[18], O.Podobrin[15], M.E.Pol[17], G.Polok[16], P.Poropat[46], V.Pozdniakov[14], M.Prest[46], P.Privitera[38], A.Pullia[27], D.Radojicic[34], S.Ragazzi[27], H.Rahmani[31], P.N.Ratoff[19], A.L.Read[32], M.Reale[52], P.Rebecchi[18], N.G.Redaelli[27], M.Regler[50], D.Reid[7], P.B.Renton[34], L.K.Resvanis[3], F.Richard[18], J.Richardson[21], J.Ridky[10], G.Rinaudo[45], A.Romero[45], I.Roncagliolo[11], P.Ronchese[35], E.I.Rosenberg[1], E.Rosso[7], P.Roudeau[18], T.Rovelli[5], W.Ruckstuhl[30], V.Ruhlmann-Kleider[39], A.Ruiz[41], K.Rybicki[16], H.Saarikko[13], Y.Sacquin[39],

G.Sajot[12], J.Salt[49], J.Sanchez[25], M.Sannino[11], S.Schael[7], H.Schneider[15], M.A.E.Schyns[52], G.Sciolla[45], F.Scuri[46], A.M.Segar[34], A.Seitz[15], R.Sekulin[37], R.Seufert[15], R.C.Shellard[36], I.Siccama[30], P.Siegrist[39], S.Simonetti[11], F.Simonetto[35], A.N.Sisakian[14], G.Skjevling[32], G.Smadja[39,24], O.Smirnova[14], G.R.Smith[37], R.Sosnowski[51], D.Souza-Santos[36], T.Spassov[20], E.Spiriti[40], S.Squarcia[11], H.Staeck[52], C.Stanescu[40], S.Stapnes[32], G.Stavropoulos[9], F.Stichelbaut[7], A.Stocchi[18], J.Strauss[50], J.Straver[7], R.Strub[8], B.Stugu[4], M.Szczekowski[51], M.Szeptycka[51], P.Szymanski[51], T.Tabarelli[27], O.Tchikilev[42], G.E.Theodosiou[9], Z.Thome[47], A.Tilquin[26], J.Timmermans[30], V.G.Timofeev[14], L.G.Tkatchev[14], T.Todorov[8], D.Z.Toet[30], A.Tomaradze[2], B.Tome[20], E.Torassa[45], L.Tortora[40], D.Treille[7], W.Trischuk[7], G.Tristram[6], C.Troncon[27], A.Tsirou[7], E.N.Tsyganov[14], M.Turala[16], M-L.Turluer[39], T.Tuuva[13], I.A.Tyapkin[22], M.Tyndel[37], S.Tzamarias[21], B.Ueberschaer[52], S.Ueberschaer[52], O.Ullaland[7], V.Uvarov[42], G.Valenti[5], E.Vallazza[7], J.A.Valls Ferrer[49], C.Vander Velde[2], G.W.Van Apeldoorn[30], P.Van Dam[30], M.Van Der Heijden[30], W.K.Van Doninck[2], J.Van Eldik[30], P.Vaz[7], G.Vegni[27], L.Ventura[35], W.Venus[37], F.Verbeure[2], M.Verlato[35], L.S.Vertogradov[14], D.Vilanova[39], P.Vincent[24], L.Vitale[46], E.Vlasov[42], A.S.Vodopyanov[14], M.Vollmer[52], M.Voutilainen[13], H.Wahlen[52], C.Walck[44], F.Waldner[46], A.Wehr[52], M.Weierstall[52], P.Weilhammer[7], A.M.Wetherell[7], J.H.Wickens[2], M.Wielers[15], G.R.Wilkinson[34], W.S.C.Williams[34], M.Winter[8], M.Witek[7], G.Wormser[18], K.Woschnagg[48], A.Zaitsev[42], A.Zalewska[16], D.Zavrtanik[43], E.Zevgolatakos[9], N.I.Zimin[14], M.Zito[39], D.Zontar[43], R.Zuberi[34], G.Zumerle[35]

[1] Ames Laboratory and Department of Physics, Iowa State University, Ames IA 50011, USA
[2] Physics Department, Univ. Instelling Antwerpen, Universiteitsplein 1, B-2610 Wilrijk, Belgium
and IIHE, ULB-VUB, Pleinlaan 2, B-1050 Brussels, Belgium
and Faculté des Sciences, Univ. de l'Etat Mons, Av. Maistriau 19, B-7000 Mons, Belgium
[3] Physics Laboratory, University of Athens, Solonos Str. 104, GR-10680 Athens, Greece
[4] Department of Physics, University of Bergen, Allégaten 55, N-5007 Bergen, Norway
[5] Dipartimento di Fisica, Università di Bologna and INFN, Via Irnerio 46, I-40126 Bologna, Italy
[6] Collège de France, Lab. de Physique Corpusculaire, IN2P3-CNRS, F-75231 Paris Cedex 05, France
[7] CERN, CH-1211 Geneva 23, Switzerland
[8] Centre de Recherche Nucléaire, IN2P3 - CNRS/ULP - BP20, F-67037 Strasbourg Cedex, France
[9] Institute of Nuclear Physics, N.C.S.R. Demokritos, P.O. Box 60228, GR-15310 Athens, Greece
[10] FZU, Inst. of Physics of the C.A.S. High Energy Physics Division, Na Slovance 2, CS-180 40, Praha 8, Czechoslovakia
[11] Dipartimento di Fisica, Università di Genova and INFN, Via Dodecaneso 33, I-16146 Genova, Italy
[12] Institut des Sciences Nucléaires, IN2P3-CNRS, Université de Grenoble 1, F-38026 Grenoble, France
[13] Research Institute for High Energy Physics, SEFT, P.O. Box 9, FIN-00014 University of Helsinki, Finland
[14] Joint Institute for Nuclear Research, Dubna, Head Post Office, P.O. Box 79, 101 000 Moscow, Russian Federation
[15] Institut für Experimentelle Kernphysik, Universität Karlsruhe, Postfach 6980, D-76128 Karlsruhe, Germany
[16] High Energy Physics Laboratory, Institute of Nuclear Physics, Ul. Kawiory 26a, PL-30055 Krakow 30, Poland
[17] Centro Brasileiro de Pesquisas Físicas, rua Xavier Sigaud 150, RJ-22290 Rio de Janeiro, Brazil
[18] Université de Paris-Sud, Lab. de l'Accélérateur Linéaire, IN2P3-CNRS, Bat 200, F-91405 Orsay, France
[19] School of Physics and Materials, University of Lancaster, Lancaster LA1 4YB, UK
[20] LIP, IST, FCUL - Av. Elias Garcia, 14-1°, P-1000 Lisboa Codex, Portugal
[21] Department of Physics, University of Liverpool, P.O. Box 147, Liverpool L69 3BX, UK
[22] LPNHE, IN2P3-CNRS, Universités Paris VI et VII, Tour 33 (RdC), 4 place Jussieu, F-75252 Paris Cedex 05, France
[23] Department of Physics, University of Lund, Sölvegatan 14, S-22363 Lund, Sweden
[24] Université Claude Bernard de Lyon, IPNL, IN2P3-CNRS, F-69622 Villeurbanne Cedex, France
[25] Universidad Complutense, Avda. Complutense s/n, E-28040 Madrid, Spain
[26] Univ. d'Aix - Marseille II - CPP, IN2P3-CNRS, F-13288 Marseille Cedex 09, France
[27] Dipartimento di Fisica, Università di Milano and INFN, Via Celoria 16, I-20133 Milan, Italy
[28] Niels Bohr Institute, Blegdamsvej 17, DK-2100 Copenhagen 0, Denmark
[29] NC, Nuclear Centre of MFF, Charles University, Areal MFF, V Holesovickach 2, CS-180 00, Praha 8, Czechoslovakia
[30] NIKHEF-H, Postbus 41882, NL-1009 DB Amsterdam, The Netherlands
[31] National Technical University, Physics Department, Zografou Campus, GR-15773 Athens, Greece
[32] Physics Department, University of Oslo, Blindern, N-1000 Oslo 3, Norway
[33] Dpto. Fisica, Univ. Oviedo, C/P.Jimenez Casas, S/N-33006 Oviedo, Spain
[34] Department of Physics, University of Oxford, Keble Road, Oxford OX1 3RH, UK
[35] Dipartimento di Fisica, Università di Padova and INFN, Via Marzolo 8, I-35131 Padua, Italy
[36] Depto. de Fisica, Pontificia Univ. Católica, C.P. 38071 RJ-22453 Rio de Janeiro, Brazil
[37] Rutherford Appleton Laboratory, Chilton, Didcot OX11 OQX, UK
[38] Dipartimento di Fisica, Università di Roma II and INFN, Tor Vergata, I-00173 Rome, Italy
[39] Centre d'Etude de Saclay, DSM/DAPNIA, F-91191 Gif-sur-Yvette Cedex, France
[40] Istituto Superiore di Sanità, Ist. Naz. di Fisica Nucl. (INFN), Viale Regina Elena 299, I-00161 Rome, Italy
[41] C.E.A.F.M., C.S.I.C. - Univ. Cantabria, Avda. los Castros, S/N-39006 Santander, Spain
[42] Inst. for High Energy Physics, Serpukov P.O. Box 35, Protvino, (Moscow Region), Russian Federation
[43] J. Stefan Institute and Department of Physics, University of Ljubljana, Jamova 39, SI-61000 Ljubljana, Slovenia
[44] Fysikum, Stockholm University, Box 6730, S-113 85 Stockholm, Sweden
[45] Dipartimento di Fisica Sperimentale, Università di Torino and INFN, Via P. Giuria 1, I-10125 Turin, Italy
[46] Dipartimento di Fisica, Università di Trieste and INFN, Via A. Valerio 2, I-34127 Trieste, Italy
and Istituto di Fisica, Università di Udine, I-33100 Udine, Italy
[47] Univ. Federal do Rio de Janeiro, C.P. 68528 Cidade Univ., Ilha do Fundão BR-21945-970 Rio de Janeiro, Brazil
[48] Department of Radiation Sciences, University of Uppsala, P.O. Box 535, S-751 21 Uppsala, Sweden
[49] IFIC, Valencia-CSIC, and D.F.A.M.N., U. de Valencia, Avda. Dr. Moliner 50, E-46100 Burjassot (Valencia), Spain
[50] Institut für Hochenergiephysik, Österr. Akad. d. Wissensch., Nikolsdorfergasse 18, A-1050 Vienna, Austria
[51] Inst. Nuclear Studies and University of Warsaw, Ul. Hoza 69, PL-00681 Warsaw, Poland
[52] Fachbereich Physik, University of Wuppertal, Postfach 100 127, D-5600 Wuppertal 1, Germany

1 Introduction

The precise measurement of the B hadron lifetime is important for the study of the weak decays of the b quark and of its couplings to the u and c quarks. Several direct measurements of the average lifetime of B hadrons, τ_B, have been performed at e^+e^- and $p\bar{p}$ colliders [1]. In this paper, two different analyses are presented. The first analysis is an improvement on a previous technique [2], which used charged particle impact parameter distributions. The second analysis is based on a new technique for reconstructing secondary vertices.

These two analyses provided complementary measurements of the average lifetime of B hadrons. In the impact parameter analysis, the uncertainty of the fragmentation of the Z^0 into B hadrons was reduced compared to the vertex analysis; in the vertex analysis, the uncertainty of the charged particle tracking resolution was found to be negligible in comparison with the impact parameter analysis. The uncertainties in the measurement of the lifetime arising from the knowledge of the production fractions and branching ratios of b and c hadrons, and the uncertainty in the lifetimes of D mesons were found to be smaller in the vertex analysis. Due to the differing selection requirements of these two measurements, the number of events in common was small. Thus, the combination of these two analyses leads to a more precise measurement of the average lifetime of B hadrons.

In addition, compared to the previous DELPHI result [2], both analyses benefit from a factor of 10 increase in statistics and an improved vertex detector. This allowed a more precise reconstruction of charged particles, improving the knowledge of the systematic uncertainties associated with the measurement and increasing the sensitivity to short lived heavy flavored hadrons. Therefore, the result presented in this paper supersedes the previously published DELPHI result.

2 The DELPHI detector

The DELPHI detector has been described in detail elsewhere [3], only those components which were relevant to these analyses are discussed here.

The tracking of charged particles was accomplished with a set of cylindrical tracking detectors whose axes were oriented along the 1.23 T magnetic field and the direction of the beam. The z axis was defined to be along the axis of the magnetic field, with positive z pointing in the direction of the outgoing electron beam. The Vertex Detector (VD), located nearest the LEP interaction region, had an intrinsic resolution of 5–6 μm and consisted of three concentric layers of silicon microstrip detectors at average radii of 6.3 cm, 8.8 cm, and 10.9 cm. A beryllium beam pipe with a radius of 5.5 cm was installed in 1991, which allowed the extra layer of silicon microstrip detectors to be added at a radius of 6.3 cm. Outside the VD between radii of 12 cm and 28 cm was the Inner Detector (ID), a jet chamber giving up to 24 spatial measurements. The VD and ID were surrounded by the main DELPHI tracking chamber, the Time Projection Chamber (TPC), which provided up to 16 space points between radii of 30 cm and 122 cm. The Outer Detector (OD) at a radius of 198 cm to 206 cm consisted of five layers of drift cells. The average momentum resolution of the tracking system was measured to be $\sigma(p)/p = 0.001\ p$ (where p is expressed in units of GeV/c) in the polar region between 30° and 150°.

After alignment corrections had been applied, the resolution of the charged particle track extrapolation to the interaction region was measured using high momentum muons

from $Z^0 \rightarrow \mu^+\mu^-$ events. A value of 26 ± 2 μm for this resolution was obtained. In hadronic events, the extrapolation accuracy has been measured over the full momentum range to be $\sqrt{26^2 + 69^2/p_t^2}$ μm, where p_t is the transverse momentum of the particle with respect to the z axis and is measured in units of GeV/c [4].

3 Data Sets and Event Selection

These analyses used the data collected with the DELPHI detector during 1991 and 1992, which corresponded to a total integrated luminosity of 33.9 pb^{-1}.

In both analyses, charged particles were required to have a measured momentum, p, greater than 100 MeV/c and less than 50 GeV/c, a polar angle, θ, greater than 20° and less than 160°, a reconstructed charged particle track length of more than 20 cm, and a distance of closest approach to the centre of the beam interaction region of less than 5 cm in radius and less than 10 cm in z. Neutral particles were required to have a measured energy of at least 100 MeV and less than 50 GeV.

Hadronic events were selected which contained at least 7 charged particles, where the sum of the squared transverse momenta of these particles was greater than 9 GeV^2/c^2. Furthermore, the sum of both the momentum of charged particles and energy of neutral particles in these events was required to be greater than 16 GeV or the invariant mass of the charged particles (neglecting the mass of each particle) had to be greater than 12 GeV/c^2. After these cuts, the 1991 data contained 240 000 hadronic events and the 1992 data contained 670 000 hadronic events.

A detailed Monte Carlo simulation was needed to help identify events containing B decays and extract the physics functions (described later) used to measure the lifetime. Thus, two Monte Carlo data sets of hadronic events were generated [5] and passed through a detailed simulation of the detector. In one sample, all the B hadron lifetimes were set to 1.200 ps, except the Λ_b lifetime which was set to 1.300 ps. This corresponded to an average lifetime for B hadrons of 1.208 ps. In the other sample, the lifetimes of all B hadrons were 1.600 ps, except for the Λ_b for which it was 1.300 ps. The average lifetime of B hadrons in this sample was 1.576 ps. Another simulation was developed to model the charged particle track efficiency, position and momentum resolution of DELPHI detector. This was used to create large simulated data samples with different average lifetimes of B hadrons and fragmentation functions.

4 Impact Parameter Analysis

The impact parameter method has been widely used to extract the average lifetime of B hadrons. Using a new selection technique, the data have been enriched in $b\bar{b}$ events. This improved purity, combined with an increase in statistics, has permitted a more accurate determination of the lifetime. The following section describes the method used to extract the average lifetime of B hadrons from charged particle impact parameter distributions.

4.1 Analysis Method

The impact parameter, δ, was defined as the distance of closest approach of a charged particle to the centre of the beam interaction region, which was assumed to be the Z^0 production point. This distance was evaluated in the xy-plane, perpendicular to the beam

direction, where the average width of the beam interaction region and charged particle tracking errors were small. The shape of the interaction region was well represented by a Gaussian distribution with $\sigma_x = 145$ μm, $\sigma_y = 7$ μm in 1991 and $\sigma_x = 100$ μm, $\sigma_y = 7$ μm in 1992. In the xy-plane, the beam centre was determined with a precision of better than 15 μm for every one hundred hadronic Z^0 decays.

The thrust axis and jets were reconstructed with the JADE algorithm [5] using charged particles. The clustering parameter, y_{cut}, was set to 0.01. The jet axis was used to estimate the B hadron direction. The impact parameter of each particle in a jet was given a positive sign if the particle intersected the jet axis on the positive side with respect to the beam centre and a negative sign otherwise, as shown in Fig. 1. Resolution effects caused δ to be distributed symmetrically around zero for particles from the primary vertex. The decay products of secondary particles had a positive δ on average.

Events were required to have $|\cos(\theta_{thrust})| < 0.7$, in order to ensure that the event was contained inside the VD acceptance. Less than 3% of the events were discarded, where the beam centre was not well reconstructed. The number of hadronic events used in this analysis was 157 000 events in 1991 and 424 000 events in 1992.

To improve the sensitivity of the measurement, the data were enriched in $b\bar{b}$ events. Each event was divided into two hemispheres, defined by the plane perpendicular to the thrust axis. One of these hemispheres was used to select $b\bar{b}$ events, while the opposite hemisphere was used to determine the lifetime. This method will be described in more detail in the following section.

Impact parameters, used to measure the lifetime, were calculated for the charged particles with momentum above 3.0 GeV/c, transverse momentum with respect to the nearest jet axis above 0.8 GeV/c, and having associated measurements in the three VD layers. These requirements improved the impact parameter resolution and reduced the uncertainty on the sign of the impact parameter. After enrichment and charged particle selection, 20342 charged particles remained in the 1991 data sample and 85609 charged particles were found in the 1992 data sample.

The impact parameter distribution, $D(\delta, \tau_B)$, is the sum of the contributions from different quarks:

$$D(\delta, \tau_B) = N_{uds} D_{uds}(\delta) + N_c D_c(\delta) + N_b D_b(\delta, \tau_B),$$

where $D_{uds}(\delta)$, $D_c(\delta)$ are the impact parameter probability distributions of charged particles from u, d, s and c respectively, $D_b(\delta, \tau_B)$ is the same quantity from $b\bar{b}$ events (depending on the average lifetime of B hadrons), and N_{uds}, N_c, N_b, are the number of charged particles which originated from the different quark flavors. The value of τ_B was extracted by finding the combination of N_b, and τ_B which gave the best description of the data, while N_c was constrained by the value obtained in the simulation.

4.2 B Enrichment

Enrichment of $b\bar{b}$ events was performed by selecting a number of charged particles with a large impact parameter in one hemisphere, while the impact parameters of the charged particles in the opposite hemisphere were used to measure the B hadron lifetime. To avoid biasing the lifetime measurement the impact parameters, of particles in opposite hemispheres, must be uncorrelated. In the lifetime determination the impact parameters were measured with respect to the beam centre. The impact parameters of the charged particles used for selecting $b\bar{b}$ events were measured with respect to a hemisphere primary vertex reconstructed with no beam centre constraint and using only the charged parti-

cles from that hemisphere. According to the simulation, the hemisphere primary vertex resolution was $\sigma_x \simeq \sigma_y \simeq 200$ μm.

Events which contained less than three charged particles in the hemisphere primary vertex were rejected. In the remaining events, the impact parameter with respect to the primary vertex was calculated for charged particles with momentum above 1 GeV/c and associated measurements in at least 2 layers of the VD. A hemisphere was selected if at least some number, N, of charged particles satisfied the condition: 0.1 mm $\leq$ $|\delta|$ $\leq$ 2.0 mm. The upper limit removed part of the background due to wrongly reconstructed primary vertices, long lived particle decays, and photon conversions in the detector.

The B purity, P_B, was defined as the fraction of $b\bar{b}$ events in the selected sample. The B efficiency, ϵ_B, was defined as the fraction of $b\bar{b}$ events initially produced, within the VD acceptance, which remained in the selected sample. Both the B purity and efficiency were studied using data. Assuming the Standard Model value of $\Gamma_{b\bar{b}}/\Gamma_{had}$ and accounting for the correlation between the both hemispheres (obtained from the simulation), P_B and ϵ_B were computed by counting the number of events in which one or two hemispheres were selected.

The correlation between P_B and ϵ_B, corresponding to different values of N, is shown in Fig. 2. For this analysis, in order to maximize the purity while maintaining high efficiency, a value of $N = 2$ was chosen. The corresponding purities and efficiencies were $P_B = 0.385 \pm 0.003$, $\epsilon_B = 0.546 \pm 0.005$ in 1991, and $P_B = 0.385 \pm 0.001$, $\epsilon_B = 0.631 \pm 0.003$ in 1992, in agreement with the results extracted from the simulation for the same parameters. The average charged particle multiplicity in a B decay was measured to be 5.6 in the simulation. From the measured B purity and the charged particle multiplicity, the fraction of charged particles produced by $b\bar{b}$ events, P_B^{track}, in the sample was estimated to be 50.5 $\pm$ 0.7 %.

4.3 Average Lifetime of B Hadrons

The impact parameter probability distributions were determined by convoluting the Monte Carlo generated impact parameter distributions (physics functions) with the resolution function. The physics functions, corresponding to different values of the B hadron lifetime, were generated in the range 1.0—1.8 ps by means of a weighting procedure [2]. The Monte Carlo generated impact parameters were computed with respect to the true Z^0 production point.

The signing error on the impact parameter was dependent on the beam centre resolution, charged particle track extrapolation errors, and the uncertainty in the B hadron direction due to the jet reconstruction. In order to account for the signing error due to the uncertainty in the B hadron direction, δ was signed using the intersection point of the generated particle and the jet axis determined from the reconstructed charged particles. The signing error due to the beam centre resolution and track extrapolation errors was accounted for in the resolution function.

The impact parameter distribution of light quark events, in the data, was used to extract the resolution function. Simulation showed that light quark events could be selected if in at least one hemisphere, no charged particle with momentum above 1 GeV/c, having at least 2 associated measurements in the VD, had an impact parameter larger than 300 μm. The impact parameter distribution of the charged particles in the opposite hemisphere was used to approximate the resolution function. The simulation showed that the contribution of charged particles from B decays to the negative part of this

impact parameter distribution was about 5 %, whereas the contribution to the positive part was approximately 25 %. Therefore, only the negative part of the impact parameter distribution was used.

The impact parameter resolution was the quadratic combination of the tracking extrapolation error with the uncertainty on the Z^0 production point, $\sigma_{\rm prod}$. The following function was used to parameterize the resolution function:

$$f(\delta) = N_0 e^{-s\delta^2/2\sigma_0^2} + N_1 e^{-s\delta^2/2\sigma_1^2} + N_2 e^{-\alpha|\delta|},$$

where N_0, N_1, and N_2 were relative normalizations, σ_0 and σ_1 described the Gaussian widths, α represented the slope of the exponential tail of the function and s was a scale parameter which was allowed to vary in the lifetime fit. Several other choices for the resolution function were tried; however, this function was found to give the best description of the data.

Since the shape of the beam interaction region was an ellipse, $\sigma_{\rm prod}$ was a function of the azimuthal angle, ϕ, of the charged particle at the production point. Therefore, the lifetime fit was performed in six regions of ϕ, to improve the sensitivity of the measurement. Each region contained data from four 15° wide sectors, one from each quadrant, which mapped onto one another under reflection in the x and y axes. The values of N_0, N_1, N_2, σ_0, σ_1, and α were found by fitting the impact parameter distribution described above in each ϕ region, while holding s fixed at 1.0. The momentum spectrum of the particles used to extract the resolution function was different from the spectrum of the particles used in the lifetime determination. This distribution was also contaminated by particles coming from B decays. Therefore, the final resolution function was obtained by allowing N_2 and s to vary during the lifetime fit.

A numerical convolution of the binned physics functions with the resolution function was performed, yielding the final probability distribution. The impact parameter distribution was fitted using a binned maximum likelihood, over the range $|\delta| \leq 2$ mm. In the fit, the B hadron lifetime, the number of charged particles originating from $b\bar{b}$ decays, N_b, and the resolution parameters, N_2 and s, were allowed to vary. Since the shapes of the impact parameter distributions for the c and uds events were similar, the fraction of charged particles from $c\bar{c}$ events, N_c, was fixed to 14% of all charged particles, in accordance with predictions from Monte Carlo simulations. The number of charged particles from u, d, and s events, N_{uds}, was constrained by the difference between the total number of charged particles and the sum of N_b with N_c.

The analysis procedure was checked using the two simulated samples with average lifetimes for B hadrons of 1.208 ps and 1.576 ps. The lifetime fit reproduced the true impact parameter resolution in each of the six independent ϕ regions. The measured average lifetimes for B hadrons were 1.219 ± 0.025 ps and 1.563 ± 0.032 ps for the two simulated samples.

Data from 1991 and 1992 were fitted separately, to take into account the different detector and beam conditions. Figure 3 shows the ϕ dependence of impact parameter resolution as measured in the lifetime fit, for both the 1991 and 1992 data. The measured resolution was found to be in agreement with the known shape of the beam interaction region convoluted with the tracking extrapolation error.

The values of the B hadron lifetime and of the charged particle purity in each ϕ region are given in Table 1 and 2 for the 1991 and 1992 data. The charged particle purity was found to be in agreement with the expected value. The measured charged particle purity was sensitive to the detector conditions. Therefore, this purity was not expected to be constant in the various ϕ regions. In Fig. 4 the impact parameter distribution

Table 1: Measured Average Lifetimes of B Hadrons and charged particle purity, P_B^{track}, for the 1991 data, in each ϕ region.

ϕ region	τ_B(ps)	P_B^{track}(%)
1	1.49 ± 0.09	53.4 ± 1.8
2	1.60 ± 0.12	48.5 ± 2.4
3	1.81 ± 0.27	44.2 ± 2.4
4	1.60 ± 0.13	50.0 ± 2.9
5	1.45 ± 0.21	54.4 ± 5.9
6	1.56 ± 0.16	50.7 ± 4.4
Average	1.55 ± 0.06	49.9 ± 1.1

Table 2: Measured Average Lifetimes of B Hadrons and charged particle purity, P_B^{track}, for the 1992 data, in each ϕ region.

ϕ region	τ_B(ps)	P_B^{track}(%)
1	1.493 ± 0.055	46.3 ± 2.6
2	1.618 ± 0.075	45.2 ± 1.7
3	1.481 ± 0.050	53.6 ± 1.6
4	1.574 ± 0.050	51.6 ± 1.5
5	1.601 ± 0.055	51.6 ± 1.7
6	1.497 ± 0.062	48.5 ± 1.5
Average	1.539 ± 0.023	49.9 ± 0.7

of the 1992 data in the two ϕ regions corresponding to the smallest and largest impact parameter resolutions are shown. The average lifetime of B hadrons was measured to be 1.551 ± 0.056 ps and 1.539 ± 0.023 ps, in the 1991 and 1992 data respectively.

4.4 Systematic Uncertainties

In order to verify the robustness of the lifetime fit, the analysis was performed in different impact parameter ranges. The impact parameter distributions of positively and negatively charged particles were fitted independently. The lifetime was calculated for data samples collected during different data taking periods. No significant effect on τ_B was found.

The resolution function, determined in the lifetime fit, was found to reproduce the tracking extrapolation error and the ϕ dependence of the impact parameter resolution. The statistical contribution, to the systematic uncertainty, originating from the impact parameter resolution was evaluated by varying the resolution parameters, in the lifetime fit, within their uncertainties. The effect of changing the slope of the exponential tails α and the relative ratio N_0/N_1 of the parameterization describing the resolution function was also studied and found to give a minor contribution to the lifetime systematic uncertainty. These uncertainties were combined to give a total systematic uncertainty of $\pm$ 0.028 ps on the lifetime, due to the resolution function. Other parameterizations were also studied for the resolution function, for example the superposition of two Gaussian distributions and the superposition of two Gaussian distributions combined with a flat distribution. The observed variation of τ_B was found to be of the order of 0.04 ps, but the corresponding fit probabilities were extremely poor.

Table 3: Sources of systematic uncertainty in the measurement of τ_B, using impact parameters.

Source of Uncertainty	$\Delta\tau_B$ (ps)
Resolution Function	$\pm$ 0.028
B Decay Multiplicity	$\pm$ 0.023
B Fragmentation	$\pm$ 0.016
D Sample Composition	$\pm$ 0.015
B Baryon Content	$\pm$ 0.008
Charmed Hadron Lifetime	$\pm$ 0.008
c Fragmentation	$\pm$ 0.007
Charmed Hadron Content	$\pm$ 0.006
Total	$\pm$ 0.045

The data were divided into different ϕ and θ regions, corresponding to known detector boundaries. No systematic uncertainty resulted from the fits in these different angular regions, in either the 1991 or 1992 data.

The acoplanarity distributions of jets in the simulation and data were found to be in agreement. In order to study the systematic effects associated with the jet clustering algorithm, the difference between the reconstructed jet axis and secondary vertex direction in the $R\phi$ plane for the data and simulation has been plotted in Fig. 5. The method for reconstructing secondary vertices will be described in the next section. The agreement between the simulation and data in this figure implied that the systematic effects due to clustering effects and impact parameter signing were negligible.

The average charged decay multiplicity in B decay was varied according to the uncertainty of the OPAL measurement [6]. The effect of the uncertainty in the b and c quark fragmentation was estimated by varying the mean fraction of beam energy carried by the B [7] and c hadrons [8]. The systematic uncertainty due to the relative abundance of different charmed hadron species was computed by varying by $\pm$ 30% the ratio between the number of $D^{\pm}$ and the number of D^0 and $D_s^{\pm}$ in the B hadron decays [9] and in the fragmentation of the charm quark. The systematic effect due to the uncertainty on charmed hadron lifetime was estimated by changing the average lifetime by 2.5% [9]. The fraction of charged particles originating from charmed decays was varied by $\pm$ 8.2% [10] in order to determine the systematic variation due to the charmed hadron content. The systematic uncertainty due to the unknown fraction of B baryons was studied by removing and doubling the number of decays arising from B baryons in the simulation. The uncertainties associated with the lifetime for each of these effects are listed in Table 3.

A total systematic uncertainty of $\pm$ 0.045 ps on the measured lifetime was obtained by adding all the contributions in quadrature.

5 Secondary Vertex Analysis

Most previous measurements of the B hadron lifetimes have been based on impact parameter methods. In these methods there was no explicit reconstruction of the decay point of the B hadron. At LEP, a 35 GeV B meson will travel, on average, 3 mm before decaying. Using the high precision vertex detector, it was possible to reconstruct secondary decay vertices and explicitly measure the projected decay distribution. This

section describes a method developed to find secondary vertices in hadronic events at DELPHI and how these vertices were used to extract an average lifetime for B hadrons.

5.1 Secondary Vertex Identification

The procedure to find secondary vertices consisted of two parts. The first part was to define which charged particles belonged to candidate vertices. The second part was to refine these vertices by removing mis-associated charged particles and measuring the properties of the remaining candidate vertices.

As the determination of the B hadron lifetime was dependent upon accurate spatial measurements in the $R\phi$-plane, the following conditions were imposed on the charged particle tracks. In order to minimize the effect of multiple Coulomb scattering, it was required that all charged particles had a momentum above 1.0 GeV/c. To ensure the charged particles were well reconstructed, their polar angle was restricted to $45° \leq \theta \leq 135°$ and each reconstructed charged particle had to be associated with measurements in at least two layers of the VD.

To find the initial candidate vertices, each reconstructed charged particle track was paired with every other charged particle and the intersection points for these charged particles were computed. Pairs of charged particles were rejected if: the charged particles did not intersect in the $R\phi$-plane, both charged particles were not in the same hemisphere as the intersection point, the intersection point lay within three standard deviations of the beam centre, or if the radial distance of the intersection point to the beam centre was greater than 5 cm.

The remaining intersection points were clustered into candidate vertices based on the separation between each pair of intersection points. Intersection points were *linked* if the distance, d, between the points in the $R\phi$-plane divided by the error, Δd, was such that $d/\Delta d < 1.0$. Links were not permitted between pairs of intersection points in opposite hemispheres or between intersection points where the sum of the momenta (for the pair of charged particles associated with each intersection point) pointed in opposite directions. An intersection point was allowed to belong to only one vertex, but a charged particle could belong to more than one intersection point and thus more than one candidate vertex.

The candidate vertices were refined to remove wrongly associated charged particles and hence improve the secondary vertex resolution. For each candidate vertex (i) the average intersection point ($< \vec{v}_i >$) was computed. This was used as a reference point in the following iterative procedure. For each candidate vertex a more precise vertex position was computed by minimizing

$$\chi^2 = \sum_j (\frac{\delta_j}{\Delta\delta_j})^2 \equiv \sum_j \beta_j^2$$

where δ_j was the distance of closest approach of the charged particle j to the vertex v_i (in the $R\phi$-plane), and $\Delta\ \delta_j$ was the associated error. A charged particle was removed from the vertex if $\beta_j > 2.5$. If any charged particle was removed then a new vertex position was calculated and this process repeated until no further charged particles could be removed.

In order to minimize the number of charged particles coming from the primary vertex, that were associated with the secondary vertex, the value of β_j was compared to the corresponding value β'_j, calculated with respect to the beam centre. If $\beta'_j < \beta_j$ then charged particle j was removed from vertex i. For vertices that were close together

there was a possibility that the clustering algorithm had not assigned the correct charged particle to the correct vertex. If the distance between any two vertices was less than 2.5 σ, where σ was the error on the vertex separation, charged particles in common between these two vertices were allocated to the vertex i for which β_j with respect to $< \vec{v}_i >$ was smaller. If one or more charged particles were removed from any vertex this procedure was repeated.

Candidate vertices that contained three or more charged particles were considered to be secondary vertices. The invariant mass, momentum, energy, and errors on the position of $\vec{v}_i$ were then calculated. In order to check the reliability of the reconstructed secondary vertices the simulations were used. The resolution in the $R\phi$-plane for the reconstructed vertices was found to be 479 $\pm$ 11 μm.

5.2 B Enrichment

To study the flavor dependence of the vertex reconstruction algorithm, events were generated for a range of different B hadron lifetimes. In order to investigate the relation between B purity and efficiency, the effect of the following variables was studied: the number of charged particle tracks in a reconstructed vertex (v_{mult}), the radial distance (R) of the reconstructed vertex position from the beam centre, and the mass (m_{vmax}) of the heaviest reconstructed vertex in the event. The B efficiency, ϵ_B, was defined as the fraction of $b\bar{b}$ events initially produced (no restrictions were made on detector acceptance) which remained in the selected sample.

Vertices associated with random charged particle crossings were a source of vertex contamination. It was possible to reduce this background by requiring $v_{mult} \geq 4$. Another source of background was vertices at low R, which were found to contain particles from the primary vertex. In order to reduce this background, it was necessary to select vertices with $R > 1$ mm. The correlation between efficiency (defined over 4π) and purity is shown in Fig. 6 as a function of R and the B lifetime.

The distribution of m_{vmax} for the data is shown in Fig. 7 for reconstructed vertices with $R > 1$ mm, together with the expected contribution from $b\bar{b}$ events and the light quarks. By requiring large vertex masses it was possible to remove the light quark contamination. Figure 8 shows the correlation between efficiency and purity as a function of m_{vmax}. For events selected with $R > 1$ mm, $m_{vmax} > 1.7$ GeV/c^2 and $v_{mult} \geq 4$, the purity at $\tau_B = 1.576$ ps was 90.2 $\pm$ 0.2 % and the efficiency was 8.14 $\pm$ 0.06 %.

The decay length, L, was calculated using the measured momentum, $|\vec{P}_{vis}|$, defined to be the vector sum of the momenta of the individual charged particles associated with each vertex and transverse momentum, $P_{tvis} = \sqrt{P_{xvis}^2 + P_{yvis}^2}$, of the vertex. Then

$$L = R \frac{|\vec{P}_{vis}|}{P_{tvis}} = R/\sin\theta,$$

where θ is the angle between the line of flight and the beam axis. An additional requirement of $L > 1.5$ mm was made, to eliminate possible bias in the lifetime measurement due to variations in the efficiency as a function of L introduced by the selection criteria used to enrich the sample. This increased the purity in the simulation to 93.5 $\pm$ 0.3 % and lowered the efficiency to 7.87 $\pm$ 0.09 %. In addition to improving the purity, these selection criteria improved the reconstructed vertex resolution from 479 $\pm$ 11 μm to 301 $\pm$ 24 μm.

The purity measured using the simulation was verified with the data in two ways. First, by fitting the momentum distributions of the leptons in these events and assuming

the branching ratios for $b \rightarrow$ *lepton*, $b \rightarrow c$ and $c \rightarrow$ *lepton*, the purity was measured to be 91.9 $\pm$ 2.0 %. Second, by counting the number of events where two vertices were selected in the data, using the efficiency measured in the simulation for the background and assuming the value of $\Gamma_{b\bar{b}}/\Gamma_{had}$, it was possible to measure the purity. After accounting for correlations induced due to the detector acceptance and beam centre correlations, the purity was measured in the data to be 93.1 $\pm$ 0.3%.

5.3 Average Lifetime of B Hadrons

In a hemisphere, the B hadron vertex is expected to be the vertex closest to the beam centre. Therefore, only the two closest vertices detected in opposite hemispheres or the closest vertex (if none were detected in the opposite hemisphere) were used. Combined with the B enrichment, this additional requirement selected 4470 vertices in the 1991 data and 10972 vertices in the 1992 data.

Separating the contributions coming from the $b\bar{b}$, $c\bar{c}$ and light quark events, decay length distributions were extracted from the simulation. The L distributions for the $c\bar{c}$ and light quark events were parameterized by the sum of two exponentials. The $b\bar{b}$ signal was parameterized by a single exponential. These parameterized decay length distributions were converted into probability distributions. Using these probability distributions and the purity determined from the simulation, a likelihood fit was performed on the data to extract the slope of the exponential for the signal. This slope varied as a function of the B hadron lifetime. This variation was linear over a wide range of lifetimes. The B hadron lifetime, in the data, was determined from this linear relationship.

Independent samples of Monte Carlo events were used to check the method. The lifetimes measured for these samples were 1.205 $\pm$ 0.016 ps and 1.590 $\pm$ 0.019 ps, to be compared with the generated values of 1.208 ps and 1.576 ps. Figure 9 shows the result of the fit to the 1991 data yielding a value for the B hadron lifetime of 1.588 $\pm$ 0.025 ps. Figure 10 shows the corresponding result for the 1992 data, which measured the average lifetime of B hadrons to be 1.627 $\pm$ 0.017 ps.

5.4 Systematic Uncertainties

Inherent to this analysis was an uncertainty in the knowledge of the B hadron lifetime coming from the linear parameterization of the exponential slope as a function of lifetime. The uncertainty in this assumption comes from both Monte Carlo statistics and the choice of a linear parameterization. The errors calculated for the linear parameterization contributed an uncertainty of 0.014 ps in the measurement of the lifetime.

The purity was correlated to the lifetime through the shape of the probability distributions. Therefore, the purity was not allowed to vary in the fit to extract the lifetime. The purity was measured with an accuracy of 0.34 %. Thus, the purity was changed by $\pm$ 0.34% in the fitting procedure to find the corresponding shift in the lifetime. The systematic uncertainty in the lifetime due to the purity was found to be 0.003 ps.

The measurement of the lifetime depends on the component of momentum of the vertex along the beam direction used to compute the decay length L. To check for any possible bias in θ due to detector effects, the data were separated into six ϕ bins and $\pm z$, since the TPC which measures θ is divided in this way. The lifetimes were then computed separately in each region. A systematic shift of 0.037 ps in the average lifetime of B hadrons was observed due to a variation of the measured lifetime in ϕ in the 1992 data. For the 1991 data, this effect was not seen. This shift was observed in an area of the

detector with known problems in ϕ, but not in θ. Therefore, an uncertainty of 0.007 ps was assigned based on the known measurement uncertainty in θ and an uncertainty of 0.037 ps was attributed in the 1992 data for detector effects.

The range in decay length used to determine the lifetime was varied, both by decreasing the maximum allowed distance and by increasing the minimum required distance. If there are differences in the lifetimes of the different B species a systematic variation in the measured average lifetime should be observed as the minimum decay length is varied. The minimum decay length was varied from 1.5 mm to 7.2 mm and no systematic variation was observed. When a fit to the resulting average lifetimes as a function of minimum decay length was extrapolated to a zero minimum decay length, it yielded a value for the lifetime which differed by 0.006 ps from the quoted result. Therefore a systematic uncertainty of 0.006 ps was attributed for this effect.

The B hadron lifetime was extracted from the distribution of the decay length. The distance L is equal to $\gamma\beta c\tau_{\mathrm{B}}$ and thus depends on the momentum distribution of the B hadrons. The fragmentation of the Z^0 into B hadrons in the simulation was tuned to agree with measured LEP values [11]. The B momentum spectrum may be inferred from the distribution of P_{vis}. The ratio

$$< |\vec{P}_{vis}| >_{data} \; / \; < |\vec{P}_{vis}| >_{MC} \; = \; 1.0021 \; \pm \; 0.0023,$$

was consistent with the quoted uncertainty [7]. The distribution of $|\vec{P}_{vis}|/\mathrm{E}_{\mathrm{beam}}$ for the data and simulation and the ratio of the simulation distribution to the data is shown in Fig. 11. The shape of this distribution in the data was found to agree with the shape extracted from the simulation. The systematic uncertainty due to the fragmentation was based on the DELPHI result for the mean X_E of $0.695 \; \pm \; 0.003 \; \pm \; 0.010$ [7], where $X_E = P/E_{\mathrm{BEAM}}$.

If the production rates of b and c hadrons, the subsequent branching ratios of b hadrons into c hadrons and the lifetimes of the c hadrons in the simulations were different than those in the data, this could affect the measurement of the average lifetime of B hadrons. The production rates of b and c hadrons and the subsequent branching ratios of b hadrons into c hadrons were varied within the uncertainties of their measured values [9]. The lifetimes of the c hadrons were varied independently for both the D^0 and $\mathrm{D}^{\pm}$ by $\approx \pm 2\%$ [9] and the D_s by $\approx \pm 7\%$. The combined systematic uncertainty, due to these effects, on the average lifetime of B hadrons has been estimated to be 0.010 ps.

The measured distance, L, was distorted by the association of charged particles from cascade c decays as well as intrinsic detector resolution. The radial shifts of the vertex position were studied in the simulation. The difference between the measured radial distance R and the generated radial distance R_{phys} is given by $\rho \; = \; R_{phys} \; - \; R$. The resolution for ρ was found to be $301 \; \pm \; 24$ μm and peaked near zero. A tail observed at negative values of ρ was attributed to charged particles from subsequent cascade decays moving the vertex position radially outwards, by an average of 95 ± 17 μm. The distribution of the *pull*, defined to be $\rho/\delta\rho$, was found to have a central Gaussian contribution with width $1.03 \; \pm \; 0.09$, consistent with an expected width of 1.0. The data were selected based on the error distribution of L, $\Delta \; L$, in order to check if there were any systematic biases due to measurement uncertainty and resolution. The lifetime was recalculated and the maximum change of 0.005 ps was attributed as the systematic uncertainty due to the choice of $\Delta \; L$.

In the following paragraphs, several additional sources of systematic uncertainty are described. These sources were found to have no statistically significant contribution to the determination of the average lifetime of B hadrons, but are described here for completeness.

Table 4: Systematic sources of uncertainty in the measurement of τ_B.

Source of Uncertainty	$\Delta\tau_B$ (ps)
Detector Effects (1992)	$\pm$ 0.037
B Fragmentation	$\pm$ 0.024
Monte Carlo Statistics	$\pm$ 0.014
Cascade c Decays	$\pm$ 0.010
$\Delta\theta$	$\pm$ 0.007
Fit Range	$\pm$ 0.006
ΔL	$\pm$ 0.005
B Purity	$\pm$ 0.003
Total (1991)	$\pm$ 0.032
Total (1992)	$\pm$ 0.049

The data were selected based on the χ^2 probability of the vertex fit as a systematic check of the lifetime. The resulting changes in the measured lifetime were less than the uncorrelated changes in the statistical uncertainty.

The efficiency for reconstructing a B vertex was measured as a function of decay length in the simulation. The lifetime was only sensitive to changes in the efficiency versus decay length, in particular differences between the data and simulation. The variation in the efficiency as a function of L in the simulation was found to agree well with the variation measured from the data. This shape was defined by the vertex position resolution and also by charged particle reassociation.

The vertex resolution was measured in the data and simulation. This was done by removing the charged particle with the largest p_t (with respect to the vertex direction) from the vertex and recomputing the vertex position. The impact parameter of this charged particle was then calculated with respect to the recomputed vertex position. The resolution could then be measured in the data, relative to the simulation, by measuring the width of this impact parameter distribution. The width of this distribution as a function of L was found to be in good agreement with the width of the same distribution measured in the simulation.

Reassociation of charged particles from the secondary vertex to the beam centre sometimes causes the true secondary charged particles to be reassociated with the beam centre, thus causing the vertex to be lost. These reassociated charged particles were defined to be charged particles not associated to the secondary vertex but having a small impact parameter with respect to the secondary vertex position. The average number of these charged particles as a function of decay length is a measure of the efficiency for reconstructing a vertex as a function of decay length. The number of reassociated charged particles as a function of decay length was measured in both the simulation and data and found to agree well within the statistics. Therefore, no systematic uncertainty to the lifetime was attributed due to the shape of the efficiency.

The parameters, which control the shape of the background, were changed by their uncertainties. No significant change in lifetime was found. Also no significant change in lifetime was observed for different selections of vertex multiplicity or the vertex charge, defined as the total charge of the particles associated to the vertex.

The total systematic uncertainties of $\pm$ 0.032 ps (1991) and $\pm$ 0.049 ps (1992) were calculated by adding in quadrature all the uncertainties summarized in Table 4.

5.5 Cross-Check of the Vertex Analysis

A second technique was developed and used as a cross-check of the vertexing analysis. This method used all charged particles with momentum greater than 1 GeV/c, which were found in the two most energetic jets. A primary vertex was then reconstructed for each event. The impact parameter of the charged particles, δ, was defined with respect to the reconstructed primary vertex and σ_δ was defined to be the error on δ. A secondary vertex search was initiated if at least two charged particles were found to have the ratio $r_\delta = \delta/\sigma_\delta$ greater than two. Charged particles were included in the secondary vertex if $r_\delta > 2$, or the impact parameter with respect to the candidate vertex was less than 1 mm and smaller than that with respect to the primary vertex. The vertex was accepted if its χ^2 probability was bigger than 0.1%. If this last condition was not fulfilled, the particle giving the largest contribution to the χ^2 was removed and the χ^2 probability recomputed.

In order to increase the B purity, a selection of events with two vertices was made. The vertex of the jet used in the lifetime analysis was required to have a radial distance R with respect to the reconstructed main vertex larger than 1 mm, a visible mass larger than 1 GeV/c^2, and an angle between the direction to the vertex and the jet direction smaller than 10°. The secondary vertex of the opposite jet was used to enrich the sample of $b\bar{b}$ events. This vertex was required to have R larger than 0.6 mm and a visible mass larger than 0.8 GeV/c^2. In simulation, this selection was found to give an event sample with a purity of 97.6 ± 0.2%, and selected 3669 vertices in the 1991 data.

The proper time, t_{prop}, was then estimated from R, by assuming that the polar angle of the B was given by the jet direction and estimating the boost from the mean X_E measured by DELPHI. Short lived particles have a small probability to be detected in this technique. To overcome this deficiency, the minimum detectable time, t_{min}, was evaluated on an event by event basis and the lifetime was expressed in terms of the difference between t_{prop} and t_{min}. A maximum likelihood fit was then performed to this distribution and a result of 1.58 ± 0.03 ps was found. The result of the fit and the distribution of these vertices is shown in Fig. 12. The uncorrelated systematic uncertainties, for this analysis compared to the previous analysis, have been estimated to be 0.04 ps. The lifetime result presented in this section was found to be consistent with the aforementioned 1991 result.

6 Conclusions

Two analyses, measuring the average lifetime of B hadrons, have been performed on the 1991 and 1992 DELPHI data. The first analysis used charged particle impact parameter distributions to find a result for the average lifetime of B hadrons of

$$\tau_B = 1.551 \pm 0.056 \pm 0.045 \text{ ps (1991)},$$

$$\tau_B = 1.539 \pm 0.023 \pm 0.045 \text{ ps (1992)},$$

and

$$\tau_B = 1.542 \pm 0.021 \pm 0.045 \text{ ps (1991 + 1992)}.$$

The second analysis used a new algorithm for inclusively reconstructing secondary vertices in hadronic events at DELPHI. In this analysis, the average lifetime of B hadrons was measured to be

$$\tau_B = 1.588 \pm 0.025 \pm 0.032 \text{ ps (1991)},$$

$$\tau_B = 1.627 \pm 0.017 \pm 0.049 \text{ ps (1992)},$$

Table 5: Fraction of B hadrons before and after event selection measured in the simulation for these analyses, where the lifetime for each B hadron was 1.60 ps.

B Hadron Type	Generated	Impact Analysis	Vertex Analysis
B^0	0.394	0.427 $\pm$0.005	0.405 $\pm$0.005
$B^{\pm}$	0.396	0.375 $\pm$0.005	0.395 $\pm$0.005
B_s	0.120	0.114 $\pm$0.002	0.123 $\pm$0.003
Λ_B	0.080	0.077 $\pm$0.002	0.069 $\pm$0.002
Other B Baryons	0.010	0.007 $\pm$0.002	0.008 $\pm$0.001

and

$$\tau_B = 1.599 \pm 0.014 \pm 0.035 \text{ ps } (1991 + 1992).$$

The average lifetime for B hadrons is determined by the production fractions and lifetimes of the various B hadrons. Therefore, any selection bias, in choosing events, which causes the relative fractions of the species to differ is a source of discrepancy in the measurement of the average lifetime. Table 5 lists the fraction of the various B hadrons remaining in these two analyses after applying all selection criteria, compared to the fraction of these hadrons originally produced in the simulation, assuming all the B hadrons have lifetimes of 1.60 ps.

The statistical correlation between these two analyses was computed by comparing the events used in both analyses. Only 4.7% of the events used in the vertex analysis were found to be in common with the events used in the charged particle analysis. The systematic effects from the B fragmentation, the knowledge of the production fractions and branching ratios of b and c hadrons, and the uncertainty in the lifetimes of the D mesons were considered to be correlated, whereas the other systematic effects in these two analyses where taken to be uncorrelated. Taking into account both the statistical correlations and correlations in the systematic uncertainties, the two results were combined to yield an average lifetime for B hadrons of

$$\tau_B = 1.582 \pm 0.012 \pm 0.032 \text{ ps}.$$

Acknowledgements

We are greatly indebted to our technical collaborators and to the funding agencies for their support in building and operating the DELPHI detector, and to the members of the CERN-SL Division for the excellent performance of the LEP collider.

References

[1] D. Buskulic et al. (ALEPH Collaboration), *Phys. Lett.***295B** (1992) 174;
O. Adriani et al. (L3 Collaboration), *Phys. Lett.***317B** (1993) 474;
R. Akers et al. (OPAL Collaboration), *Phys. Lett.***316B** (1993) 435;
F. Abe et al. (CDF Collaboration), *Phys. Rev. Lett.*, 71 (1993) 3421.

[2] P. Abreu et al. (DELPHI Collaboration), *Z. Phys.* **C 53** (1992) 567.

[3] P. Aarnio et al. (DELPHI Collaboration),*Nucl. Instr. and Meth.* **A 303** (1991) 233.

[4] N. Bingefors et al. *Nucl. Instr. and Meth.* **A 328** (1993) 447.

[5] LUND JETSET 7.3, T.Sjöstrand and M.Bengtsson, *Comp. Phys. Comm.***43** (1987) 367.

[6] R. Akers et al. (OPAL Collaboration), CERN-PPE/93-174, submitted to *Zeit. Phys.*

[7] P. Abreu et al. (DELPHI Collaboration), " Determination of $\Gamma_{b\bar{b}}$ and BR($b \to l$) using Semileptonic Decays ", submitted to the Europhysics Conference on High Energy Physics, Marseille, July 1993.

[8] P. Abreu et al. (DELPHI Collaboration), *Zeit. Phys.* **C 59** (1993) 533.

[9] Particle Data Group, *Phys. Rev.* **D 45** (1992).

[10] " Updated Parameters of the Z^0 Resonance from Combined Preliminary Data of the LEP experiments ", CERN-PPE/93-157 August (1993).

[11] P. Roudeau, Heavy flavour physics at LEP, in: Proc. Joint International Symposium and Europhysics Conference on High Energy Physics (Geneva, July 1991), Vol.2, eds S. Hegarty, *et al.* (World Scientific, Singapore, 1992) p 301.

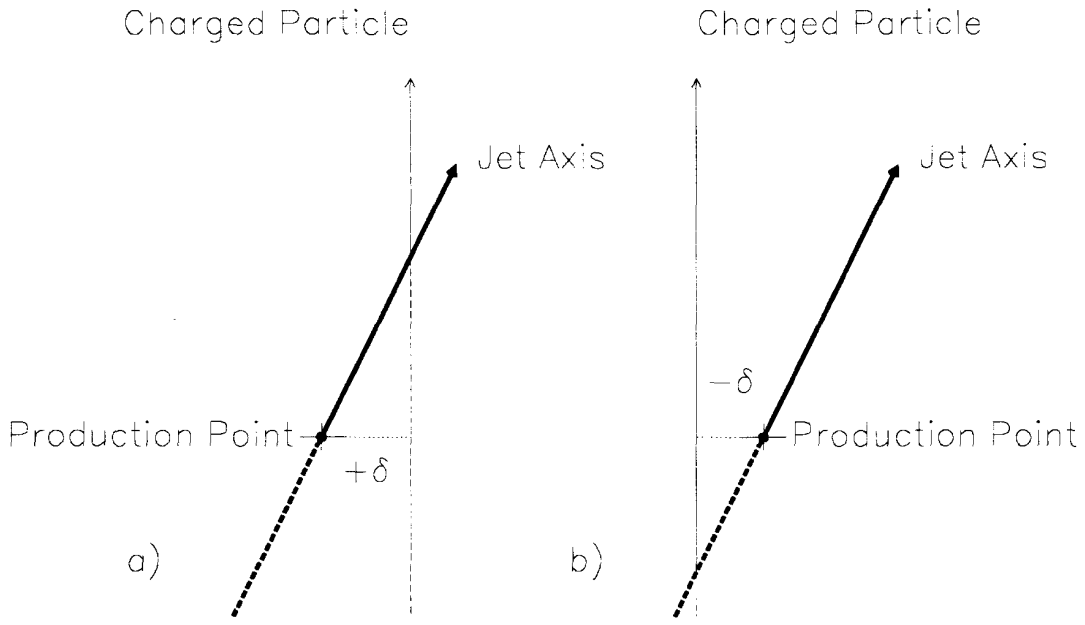

Figure 1: Schematic diagram showing the impact parameter definitions and the sign convention for the: a) positively and b) negatively signed impact parameters.

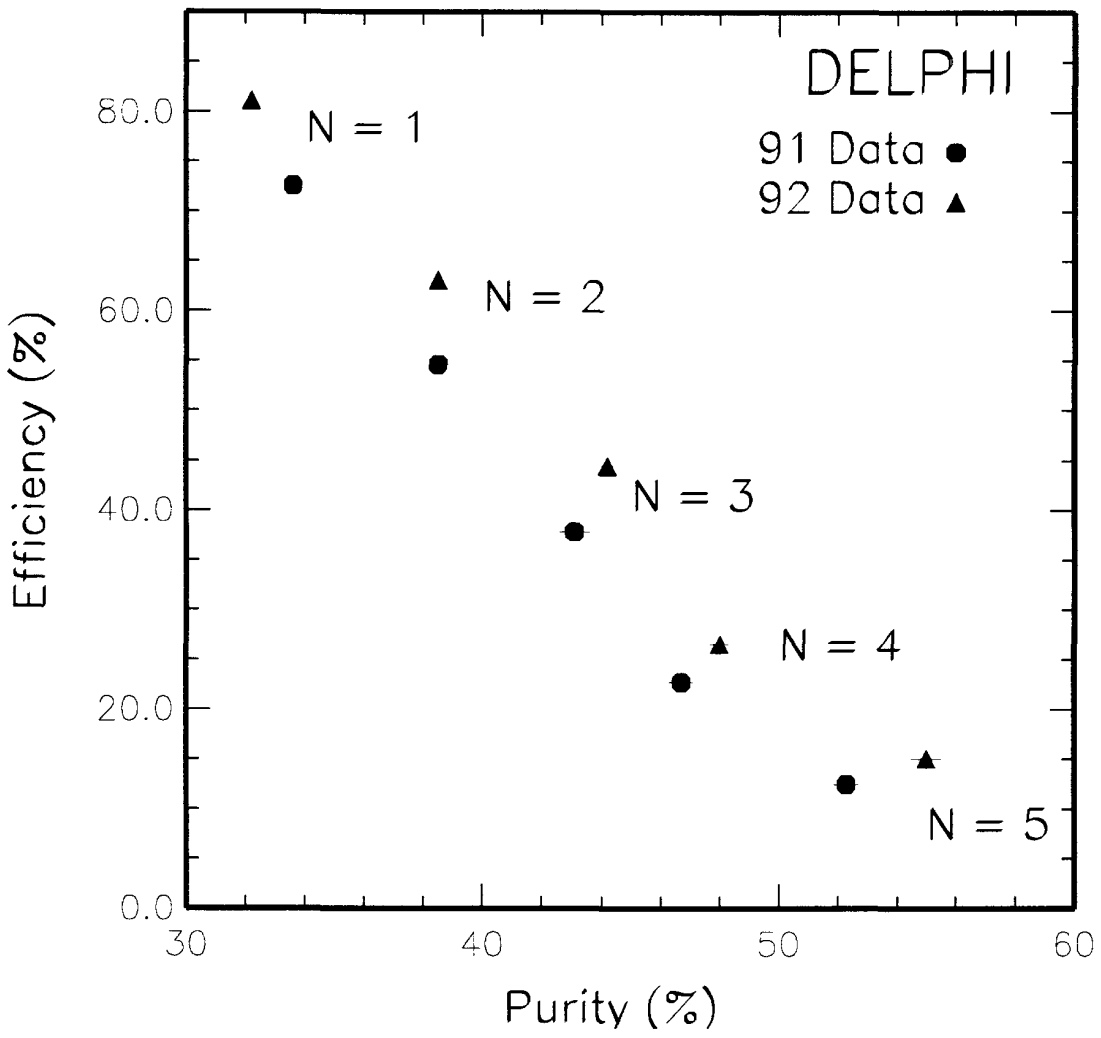

Figure 2: B efficiency versus event purity, for the impact parameter technique, in the 1991 and 1992 data.

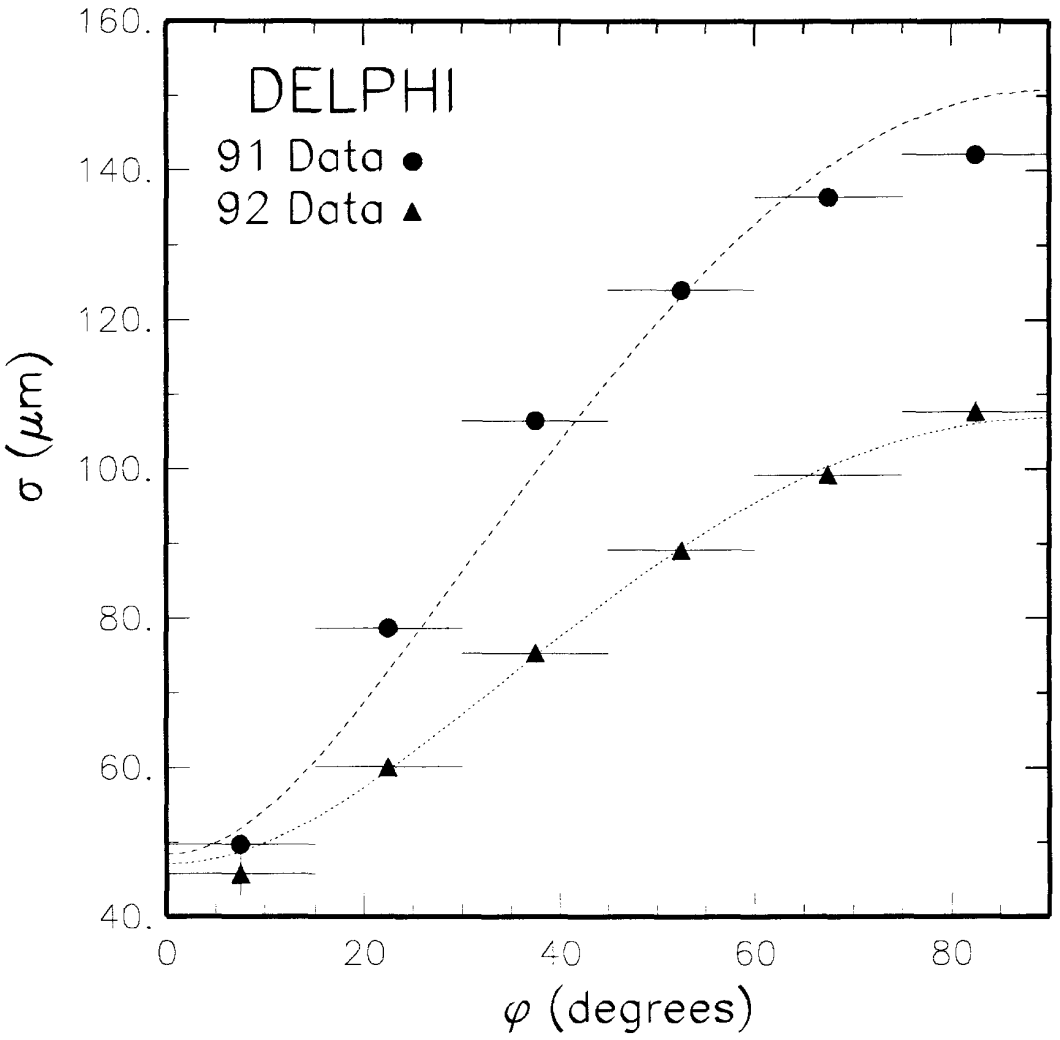

Figure 3: The measured ϕ dependence of the impact parameter resolution for the 1991 and 1992 data. The curves represent a fit to the points which reproduced the expected variation due to the shape of the beam interaction region.

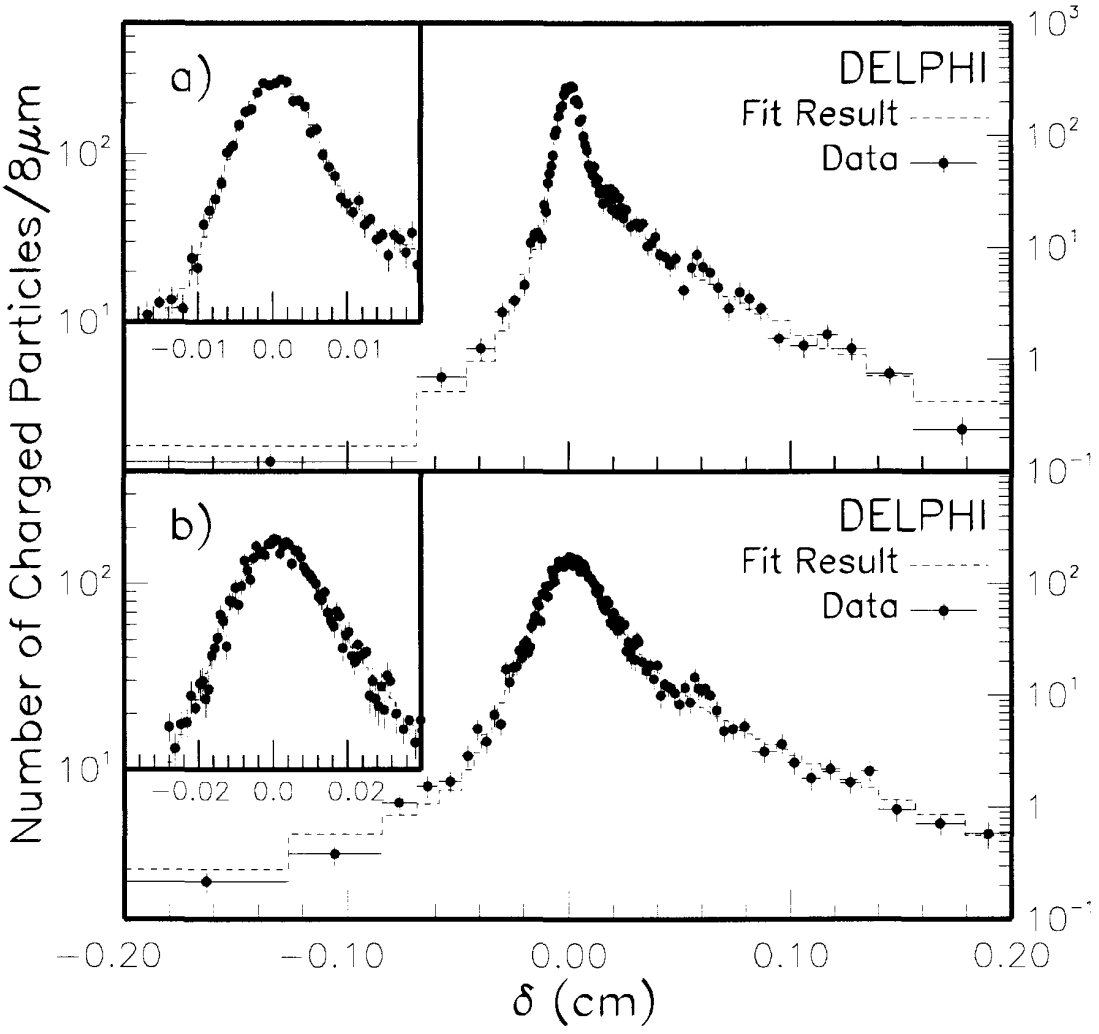

Figure 4: Impact parameter, δ, distribution of the 1992 data in ϕ regions: a) one and b) six, corresponding to the regions with the smallest and largest impact parameter resolution. The result of the lifetime fit is shown as a dashed line. The inset figures are enlargements of the central regions.

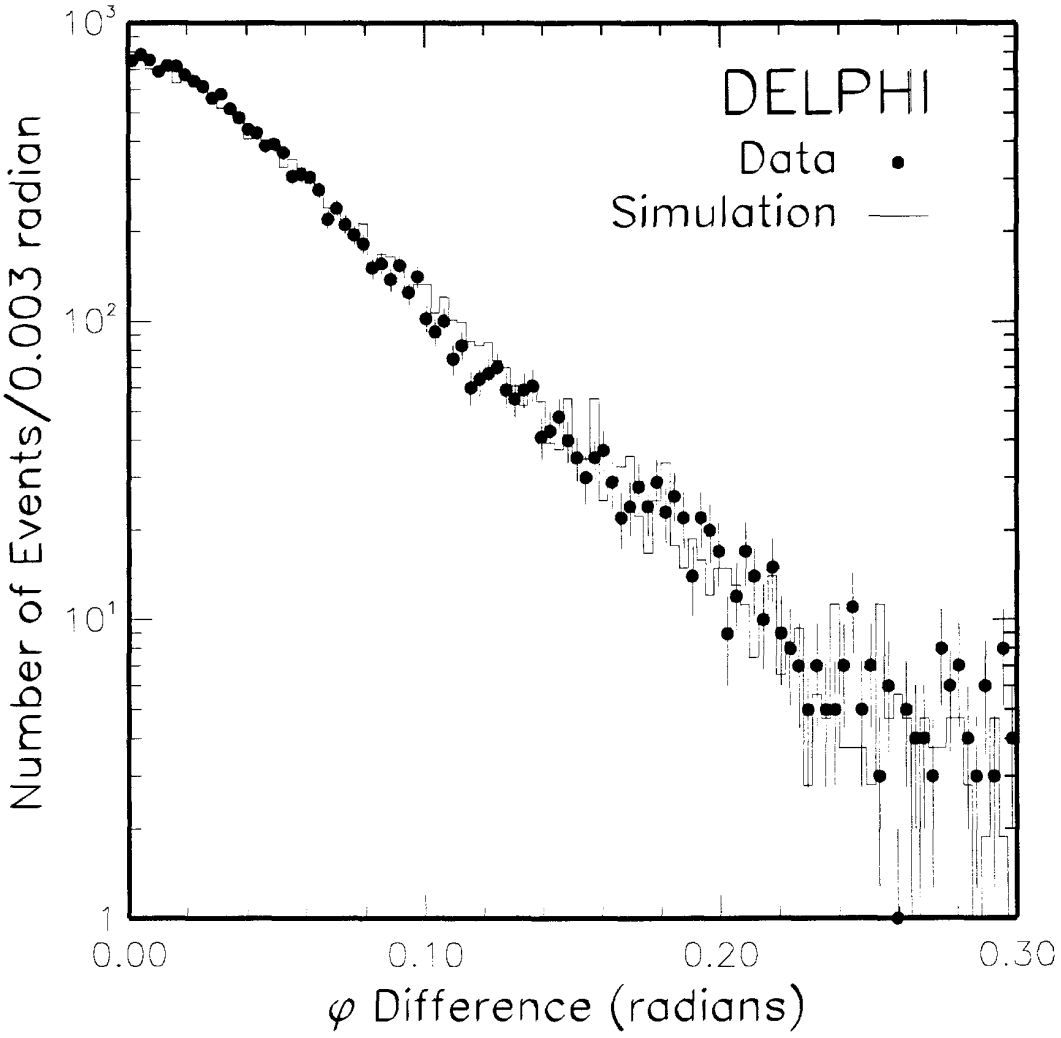

Figure 5: Difference in ϕ between the reconstructed jet axis and secondary vertex direction for the data and simulation.

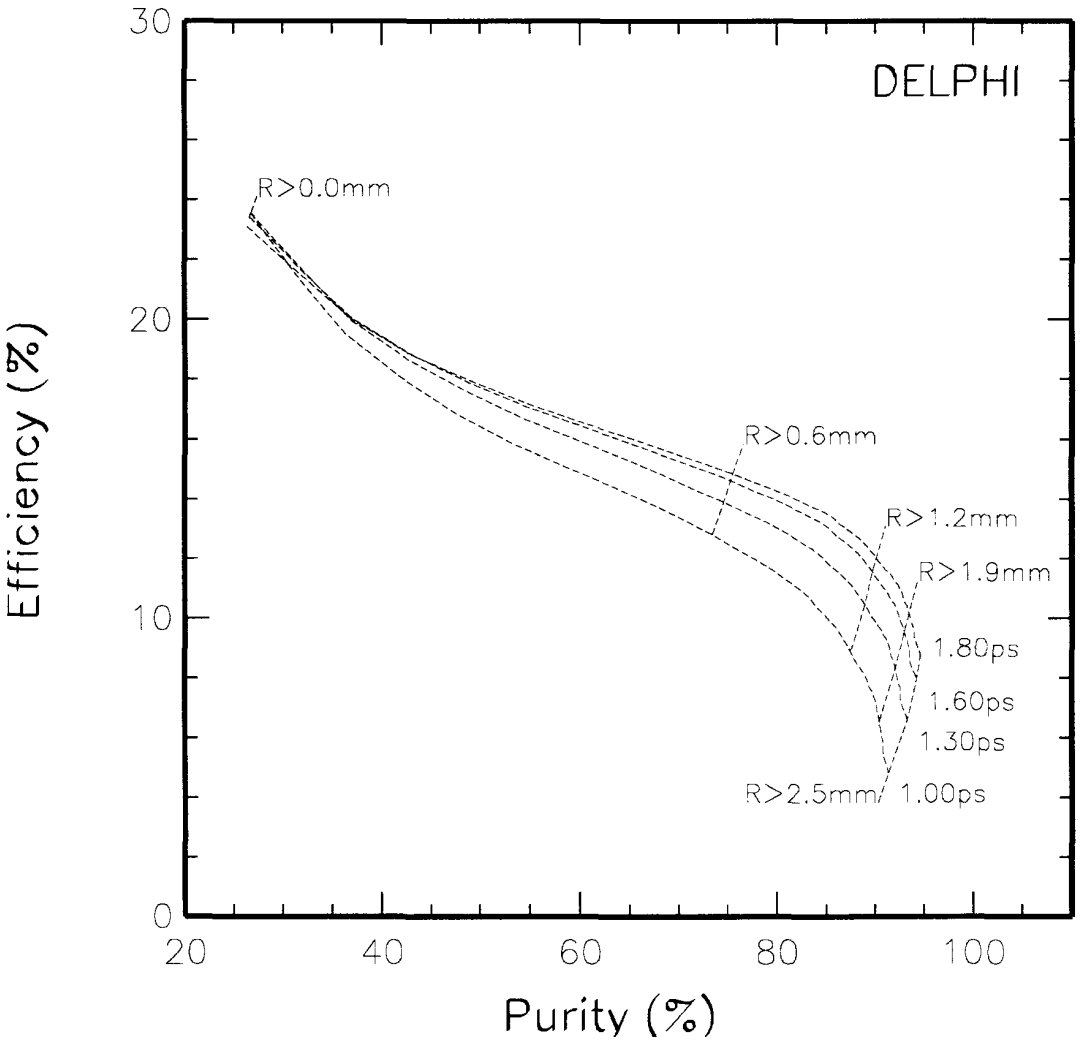

Figure 6: B efficiency versus purity, for the secondary vertex technique, as a function of the radial distance, R, (illustrated by the contour lines) for vertex multiplicity, $v_{mult} \geq 4$ and vertex mass, $m_{vmax} > 0$ GeV/c^2.

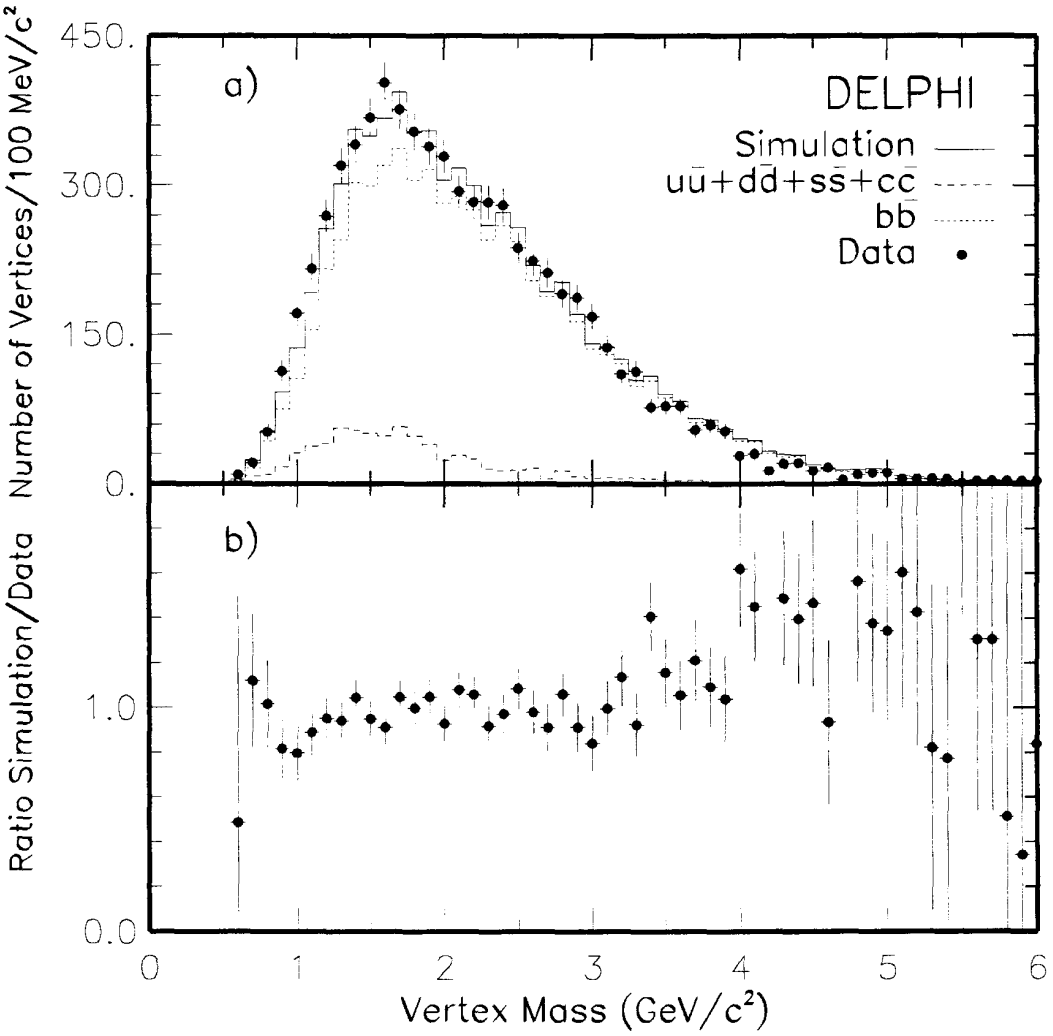

Figure 7: a) Distributions of heaviest vertex per event found with radial distance, $R > 1$ mm, and with vertex multiplicity, $v_{mult} \geq 4$ for the data and Monte Carlo simulation. Also shown are the results for the light and heavy quark flavors. b) The ratio of the simulation with respect to the data (the error bars include the statistical errors on the simulation).

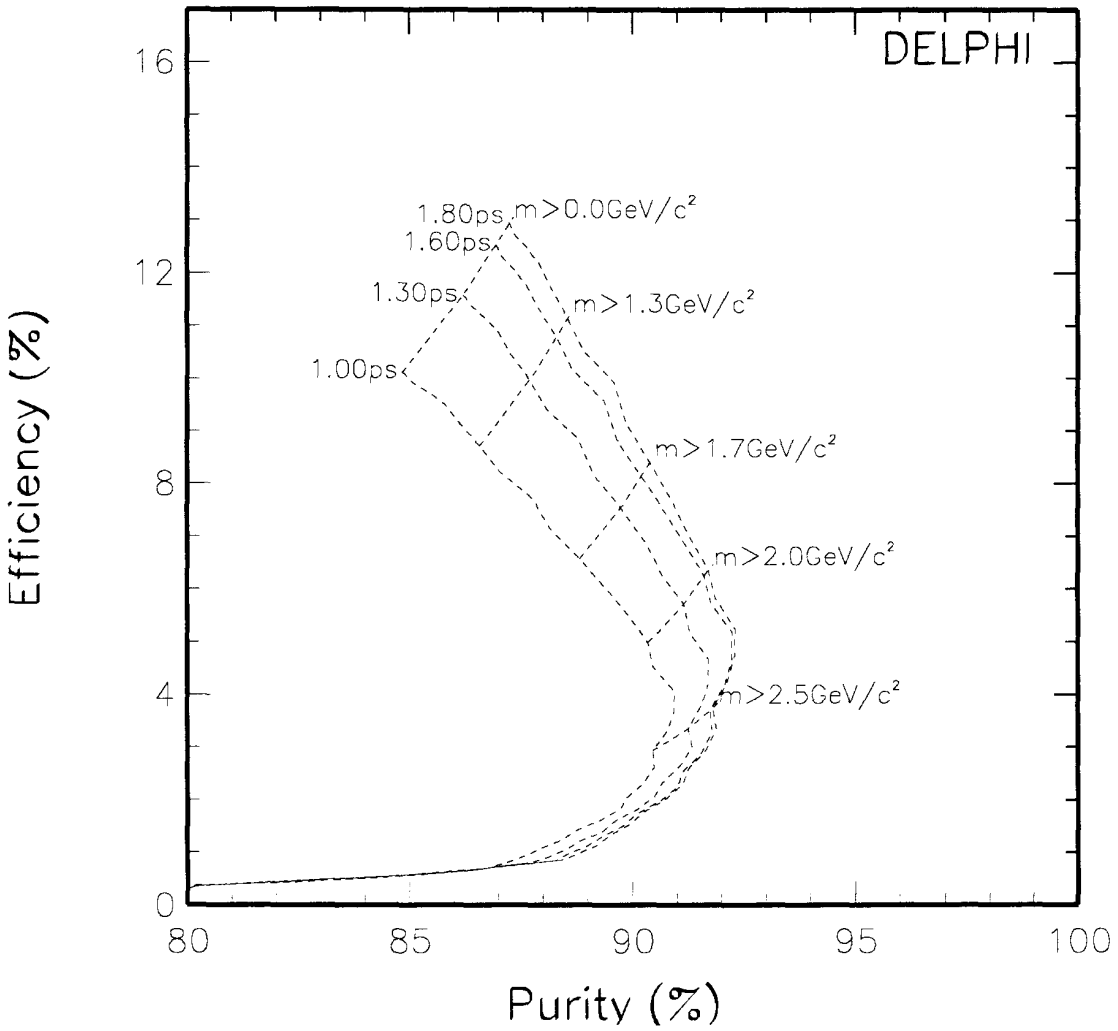

Figure 8: B efficiency versus purity, for the secondary vertex technique, as a function of the vertex mass, m_{vmax}, (illustrated by the contour lines) for vertex multiplicity, $v_{mult} \geq 4$ and radial distance, $R > 1$ mm.

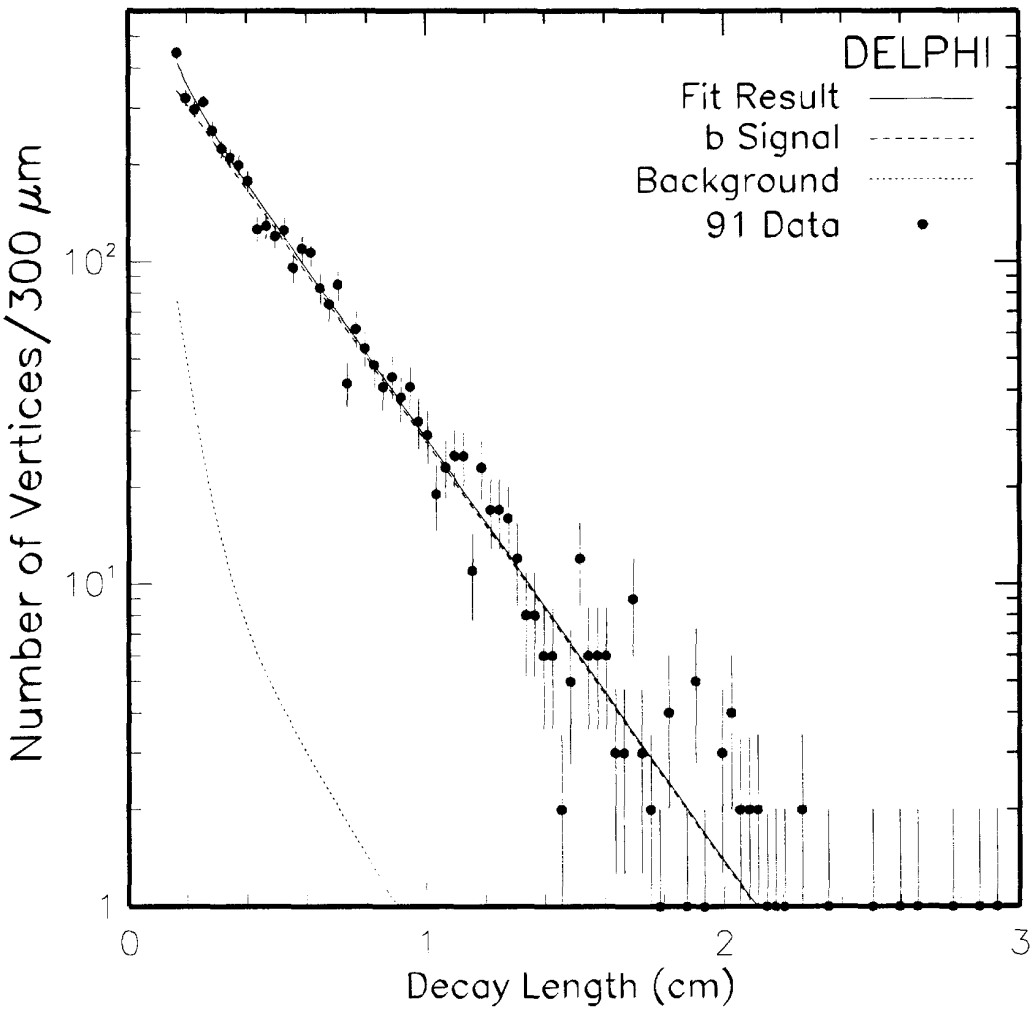

Figure 9: Result of the fit to the decay length distribution of the 1991 data, where $\tau_B = 1.588 \pm 0.025$ ps

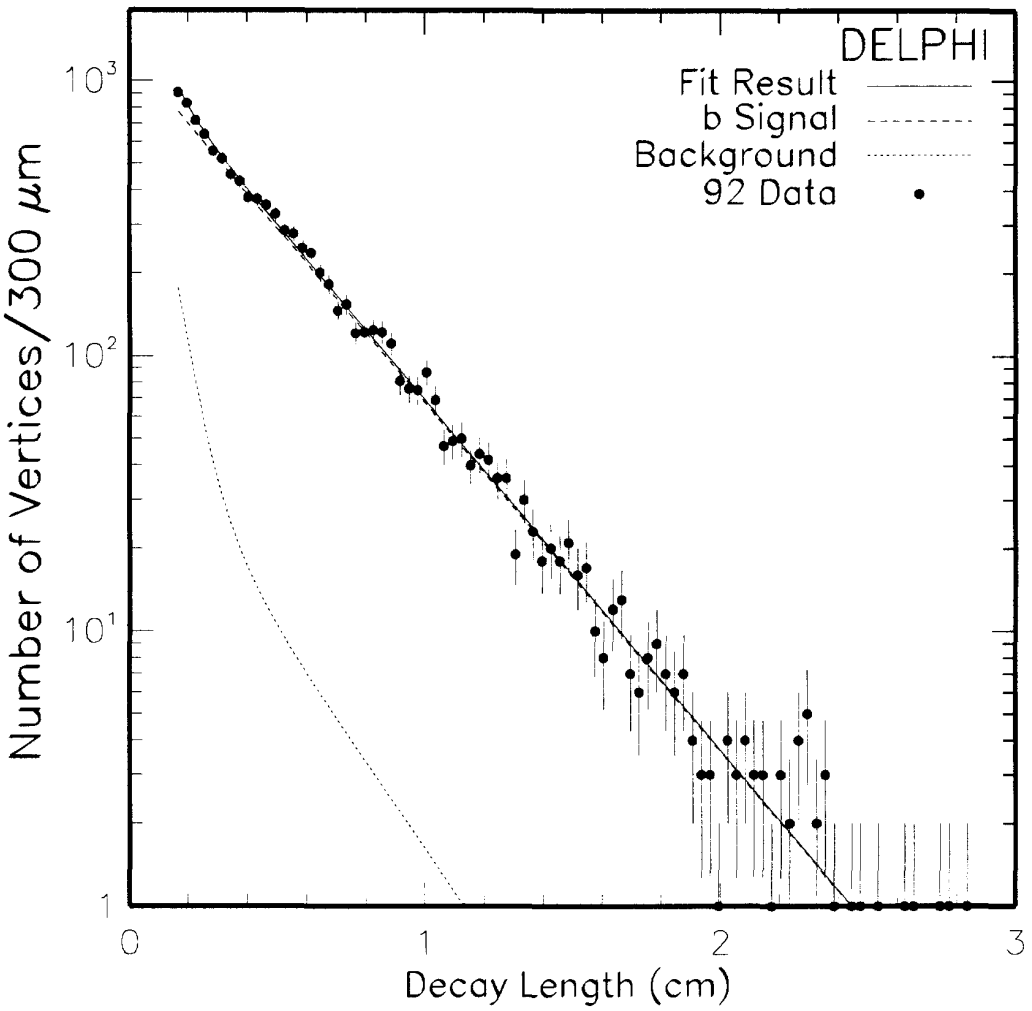

Figure 10: Result of the fit to the decay length distribution of the 1992 data, where $\tau_B = 1.627 \pm 0.017$ ps.

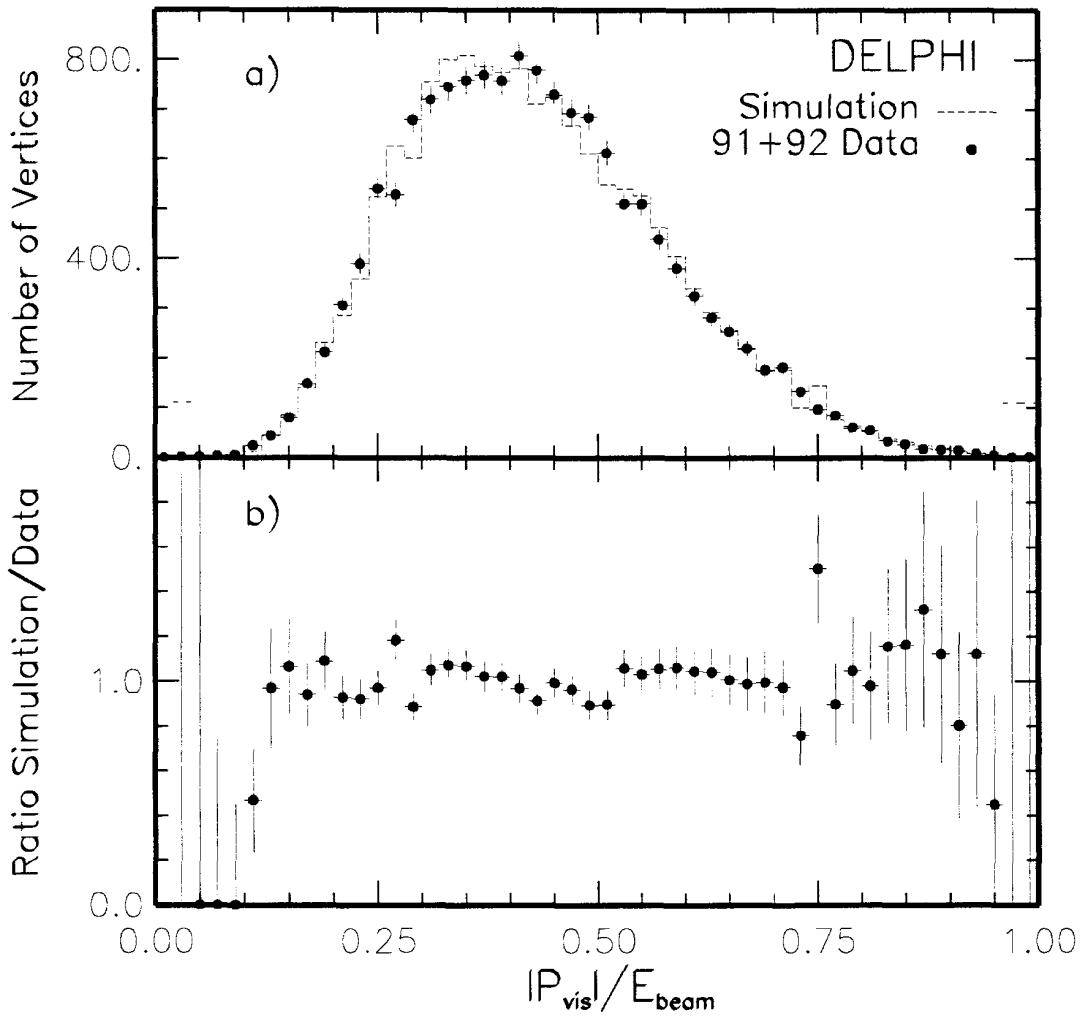

Figure 11: a) $< |\vec{P}_{vis}| > /E_{beam}$ for vertices used in this analysis and b) ratio of the simulation with respect to the data.

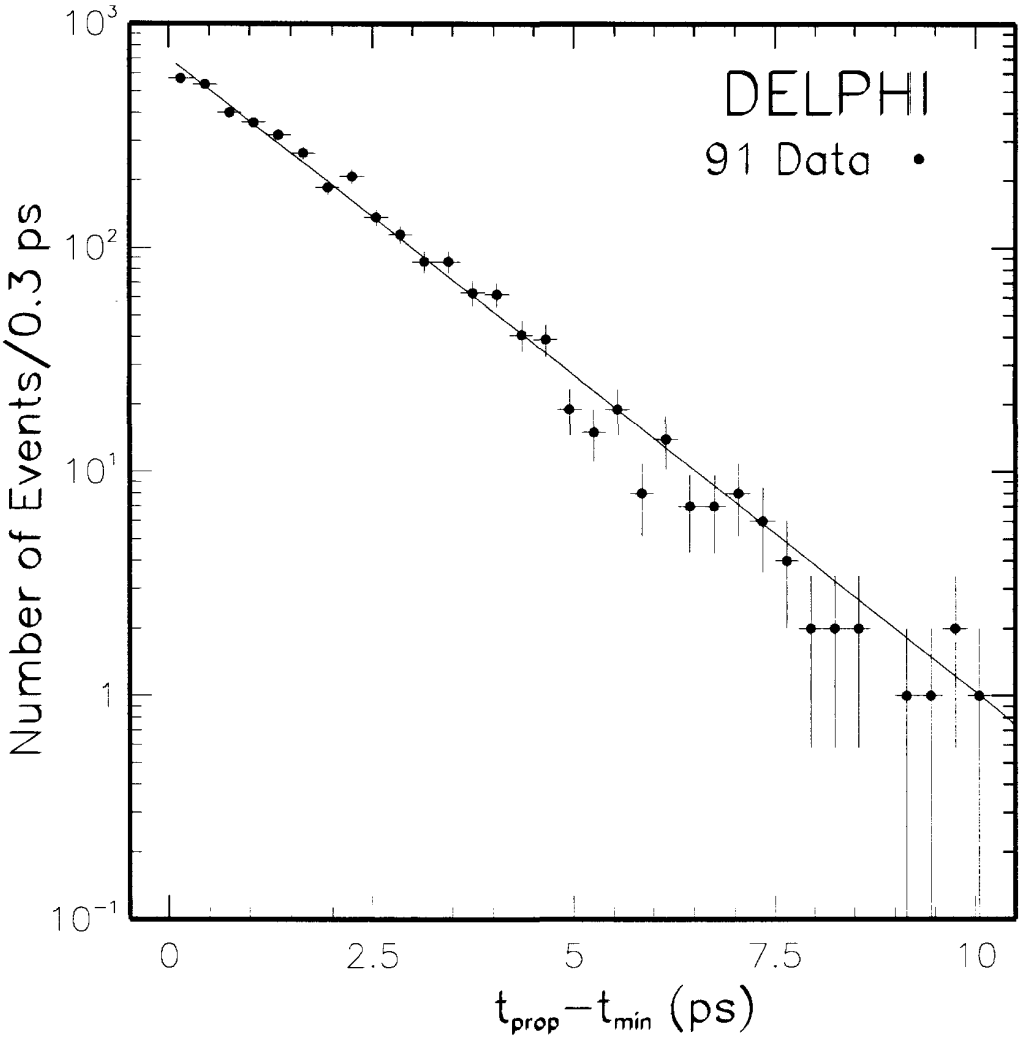

Figure 12: $t_{prop}-t_{min}$ distribution for the 1991 data.